Introduction & Literature Survey

1.1 Coordination Polymers

The area of coordination polymers has been an emerging and extremely fashonized scientific domain of material science. Coordination polymers (CPs) deals with the organic–inorganic hybrid materials, in which metal ions or clusters are linked by organic ligands *via* coordination bonds into indefinite crystal structures (Figure 1.1). The CPs show an attractive stability, polyfunctionality, adjustability and often has tunable porous structures with very large specific surface area.

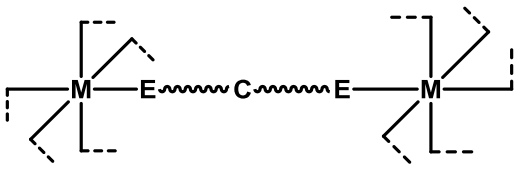

Figure 1.1 Structural representation of coordination polymer.

The synthesis of coordination polymer networks can be regarded as "construction games" where the final architecture mainly depends on the molecular building modules of ligands, solvent and metal ions. Thus, the study of geometries with diversified interactions and optimized growth processes is known as crystal engineering. In particular, the building blocks are considered as a series of reproducible molecular recognition events remarking that the overall module regulation can be imaginable along with the dimensionalities and topography resembling with single chemical entities of self–assembly and supra–molecular chemistry. The self–assembly of the CPs is based on the explicitness and complementary interactions of the molecular

units to engineer the final building block architectures. The metal ions designated as nodes and ligands are labeled as linkers or tecton in molecular architectures.

1.2 Historical Background and Discovery of Coordination Polymers

In the history of CPs, Diesbach, a Berlin colourmarker, was preparing a red pigment of cochineal red lake in 1704–1705 [Ball, 2001]. Although the method was quite simple using potash and iron sulphate but due to tiny mistake it turned into pale and consequently resulted into dark blue while increasing concentration. Diesbach synthesized Prussian blue by using extensively cheap potash with impurity of animal oil and thus Prussian blue was the first man made coordination polymer [Buser et al., 1977; Herren et al., 1908]. Within a short time period, it was commercially available as a valuable pigment and its recipe was continuously scrutinized. Later on a Russian batch reported the chemical structures of $Cd(CN)_2$ and $Zn(CN)_2$ during 2^{nd} world war; further, Rayner and Powell ascertain the chemical structures of Hoffmann clathrate $[Ni(NH_3)_2Ni(CN)_4]\cdot 2C_6H_6$ [Shugam and Zhdanov, 1945; Powell and Rayner, 1949]. Thereafter extensive study was followed by Iwamoto group further explored the research in this area. A Japanese researcher group accounted the structure of [Cu(adiponitrile)]NO_3 containing six penetrating diamond networks and the 1–D chain structure of Ag(pyrizine)NO_3 and Cu(pyrazine)$(NO_3)_2$ was established in 1966 and 1970 respectively [Miyoshi et al., 1970; Kinoshita et al., 1959]. In 1980s, the entire focus was on especially magnetic properties based molecules, which ultimately resulted a research communication in 1989 and then an extension as a full article in 1990 [Goodgame et al., 1987; Hoskins and Robson, 1990]. Successively Robson, Hoskins

and coworkers sketched an assembly based approach to engineer the coordination polymers; they described crystal structures of coordination polymers in terms of networks and employed it to develop new coordination polymers with fascinating topology and interesting properties that may be advantageous in several applications of catalysis and sensing [Wells, 1977, 1979, 1984].

Hybrid inorganic and organic materials, metal organic frameworks and coordination polymers have received much attention in recent years. These metal organic frameworks deal with the repeating unit of the organic ligand attached to a metal in an infinite array and the functioning of these materials can be controlled with the choice of their individual components. Here the assembly directed in various dimensions and volitionally chosen molecular building blocks regulate the physicochemical properties and structure of the materials up to the molecular level [Robin et al., 2004; Fromm et al., 2005]. Recently the metal–ligand coordination bond has found versatile applications in the molecular organization of various supra–molecular architectures, introducing the strength and specific directionality to the coordination bonds affiliated with metals. Metal complexes or ions and their bridging organic ligands assembled throughout the materials with various dimensionalities (1D–, 2D–, and 3D–) are referred as metal–organic frameworks (MOFs) or coordination polymers (CPs). The engineering in the design and synthesis of CPs or MOFs by the assembly of organic ligands as connecting nodes and metal ions as linkers have achieved significant attention in the family of conventional polymers and supra–molecular chemistry in the last few decades [Robin et al., 2003; Kitagawa et al., 2004].

Several CPs with high porosity and surface area persisting even upon removal of the solvent molecules has attracted a special and appealing interest because of their frontier potential applications in the broad spectrum of technologies such as catalysis, drug delivery, ion exchange, gas storage and separation. Among the various molecular building blocks studied, the organic ligands with electro negativeactive atoms are found to be highly efficient and attracting towards the construction of coordination polymers due to their stability and relative ease of functionalization due to flexibility, lone pair of electrons on heteroatoms. These organic ligands can be functionalized to build preprogrammed building blocks leading to extended structures with outstanding properties and topologies. [Moulton and Zaworotko, 2001]

1.3 Bonding in Coordination Polymers

1.3.1 Basis of Chemical Bonding in CPs

The extensive research in coordination polymers is greatly influenced by two closely associated areas, i.e. metallo–supramolecular chemistry and crystal engineering. The crystal engineering deals with the molecular packing and arrangement of molecules in the materials. This is important because molecular properties are specially governed by the spatial arrangement of molecules; thus the molecular properties can be regulated by regulating the arrangements of molecules. The interactions are stronger in coordination polymers ranging from strong hydrogen bonding to π–π interactions and van der Waals forces. The researchers are investigating the interactions that regulate the bonding architecture of coordination polymers and a net–based advancement for CPs is

found to be a significantly valid for molecular architectures associated with well–established interactions [Barnett and Champness, 2003].

Numerous concepts such as van der Waals forces, hydrogen bonding are introduced for bonding interactions in the modeling of coordination polymers; the intermolecular forces that govern the coordination synthons and assembly arrangements in CPs are hydrogen bonding and chelation. The designing of coordination polymers resembles to the supra–molecular chemistry that is to engineer the building blocks of ligands with metal ion tectons. Enormous reports have been contributed in the area of coordination polymers to define and probe the structural engineering of coordination polymers. Incorporation of metal ions leads to the achievement of required properties by regulating the metal atom positions throughout the coordination network. The organic ligands and types of metals are capable to tune the interactions in a coordination polymer, to acquire the desired functional solid material. The possible diversity in the tecton and nodes lighten the thinking of investigators for the new aspects in topologies and intriguing designing, since the crystal study is much easier with the advancement of X–ray and computational resolution techniques.

1.3.2 Interactions

The building blocks of coordination polymers are mainly based on the metal and ligand interactions, i.e. coordination bonding. Coordination bond signifies the donation of electron density from ligand to the metal. It is noteworthy that ligand behaves as a Lewis base while metal as a Lewis acid. The localised energy associated with these interactions are estimated around 40–50 $kJmol^{-1}$. A variety of weak interactions also

play a critical role in the architecture of coordination polymers.The hydrogen bonds are introduced by Steiner [Steiner, 2002]; D–H···A interaction is termed as a "hydrogen bond", if it establish a local bond, and D–H serves as proton donor to A. The variation for the strength of hydrogen bond from weak to intermediate hydrogen bond may describe with an "electrostatic van der Waals" model. Strongest hydrogen bond seldom occurs in coordination polymers and their partial covalent nature is a valid consideration. In order to understand the directional preference and strength of hydrogen bonding, a systematic study has been performed by utilizing the structural database (mainly the Cambridge Structural Database). For strong hydrogen bonding, the distance between H–A must lies in the range of 1.5–2.2 Å, while in the case of weaker hydrogen bond with D–H···A angle must lie in the range of 140–180º, 2.0–3.0 Å for the weaker C–H···O/N (with D–H···A angle in the range of 120º–180º). The localized energy for intermediate hydrogen bond lies in the range of 5 to 40 $kJmol^{-1}$. The π–π interactions have remarkable importance in the architecture of coordination polymers. Janiack studied these interactions in coordination complexes with nitrogen containing aromatic ligands (Janik, 2000). Electron cloud of aromatic rings with edge to face (C–H···π) alignment or face to face alignment (without or with offset) involves in π–π interactions. These interactions have contributions of charge transfer, van der Waal interactions, electrostatic and repulsion along with the aromatic rings stacking in an optimum way to minimize the various interactions. The geometrical parameters involved in the aromatic stacking are defined in the figure 1.2 and figure 1.3. The Cambridge structural database investigation provides the evaluation of essential factors for π–π stacking in the coordination complexes of hetero atom containing aromatic

ligands. The distance between aromatic centers in face to face interaction fall in between 3.4 to 3.8 Å with the shortest possible inclination angle between two ring planes and the offset angle ranging between 16º to 40º. The interaction energy is evaluated at 5–10 kJmol^{-1}. Metal–metal interaction can be studied on the basis of d^{10} metal cations in coordination polymers. For silver–silver interaction, the energy of the bonds is calculated as 5 kJmol^{-1}.

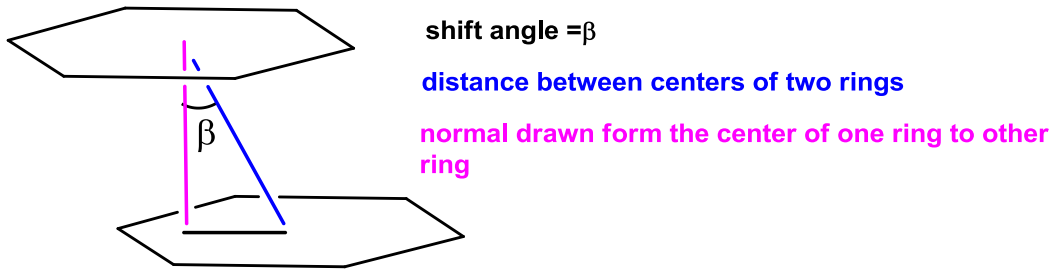

Figure 1.2 Illustration of face to face π–π interactions.

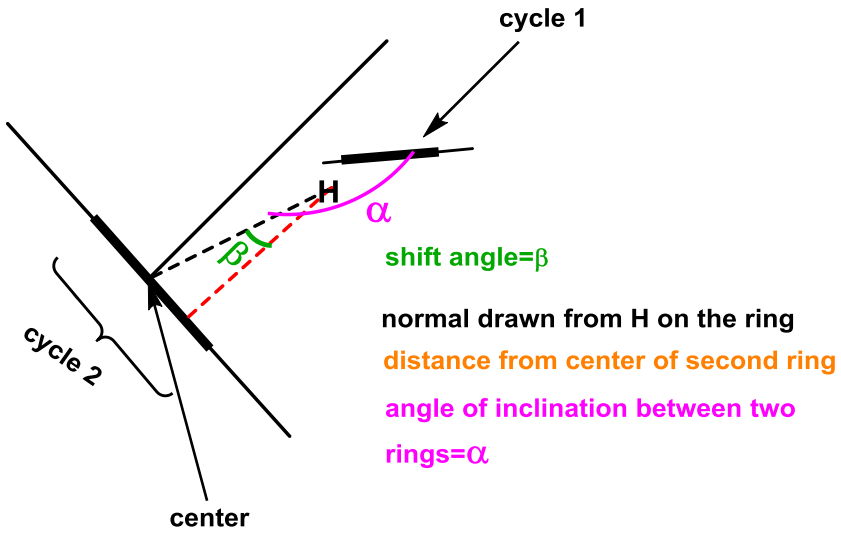

Figure 1.3 Illustration of edge to face π–π interactions.

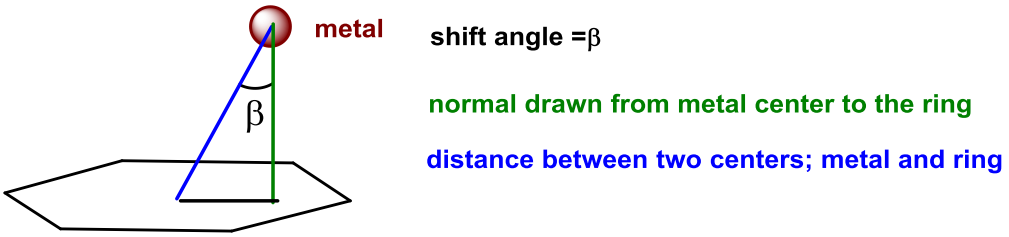

Figure 1.4 Illustration of metal–aromatic interaction.

Metal–aromatic interaction is discussed when the electron density is transferred by unsaturated ligands to metal cations. The geometrical parameters for interaction are illustrated in figure 1.4. The distance between silver–aromatic rings varies from 2.8–3.3 Å [Khlobystov et al., 2001]. The metal–aromatic ring interaction energy is estimated around 5–10 $kJmol^{-1}$.

1.3.3 Assembly

There are numerous variations in the tecton utilized for the construction of infinite arrayed coordination polymers. The metal ion employed in the fabrication of coordination polymers are in agreement with their hardness, size, and coordination geometries, e.g. square planar, trigonal planar, linear, square–pyramidal, tetrahedral, trigonal bipyramidal and trigonal prismatic etc. Most frequently used metals are transition metals and noble metals depending on their shape, size and desired properties for the potential application of coordination polymers. Ag(I) have a broad spectrum of coordination geometries varying from linear, tetragonal, square–pyramidal, tetragonal, and octahedral etc. while Cu(I) ions are generally confined in trigonal and tetragonal geometry; Cu(II) with octahedral geometry; Ni(II) in tetrahedral geometry; Pt(II) in a square planar geometry; so that enormous permutations of metal–ligand are possible.

Evidently, lanthanide ions are less frequently used for the synthesis of coordination polymers due to their excessively flexible coordination environment. The coordination number of lanthanides varies from 7–10.

In the fabrication of coordination polymers, organic ligands serve as a tecton in between metal ions. Some examples of commonly used tectons are shown in the figure 1.5 and figure 1.6. Generally, the organic ligands used in the construction of coordination polymers are divided into two categories, i.e. neutral and anionic. The other additional parameterss are nature of the ligands, rigidity, and the distance between the coordinating hands. The ligands may or may not be chiral and symmetric. In case of neutral ligands, the counter ions are also present, this influence the metal ion environment and the final architectures get involved in the possible weak interactions and serve as a guest in the voids. Further, the solvent molecules may also interact in the final construction and can serve as guest in the space of polymeric backbone.

Anionic ligands

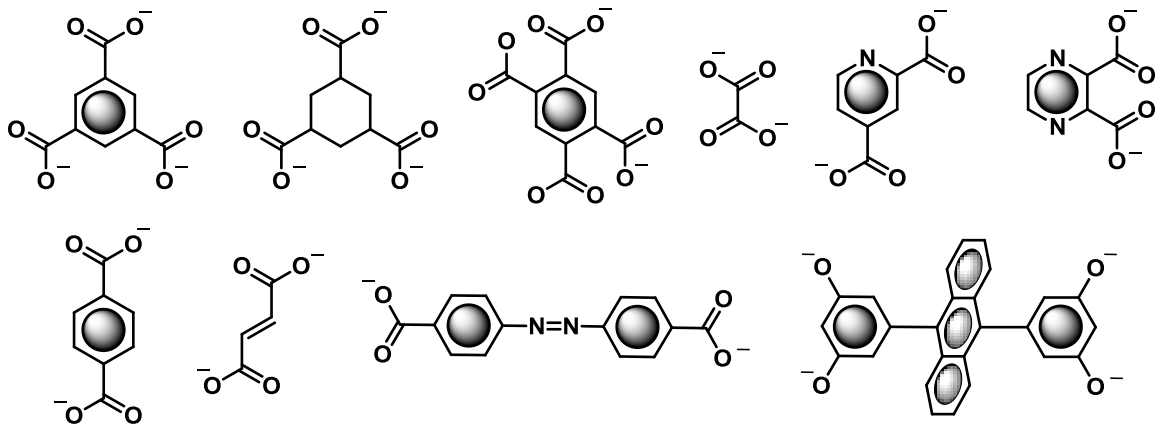

Figure 1.5 Anionic organic linkers used in the synthesis of coordination polymers.

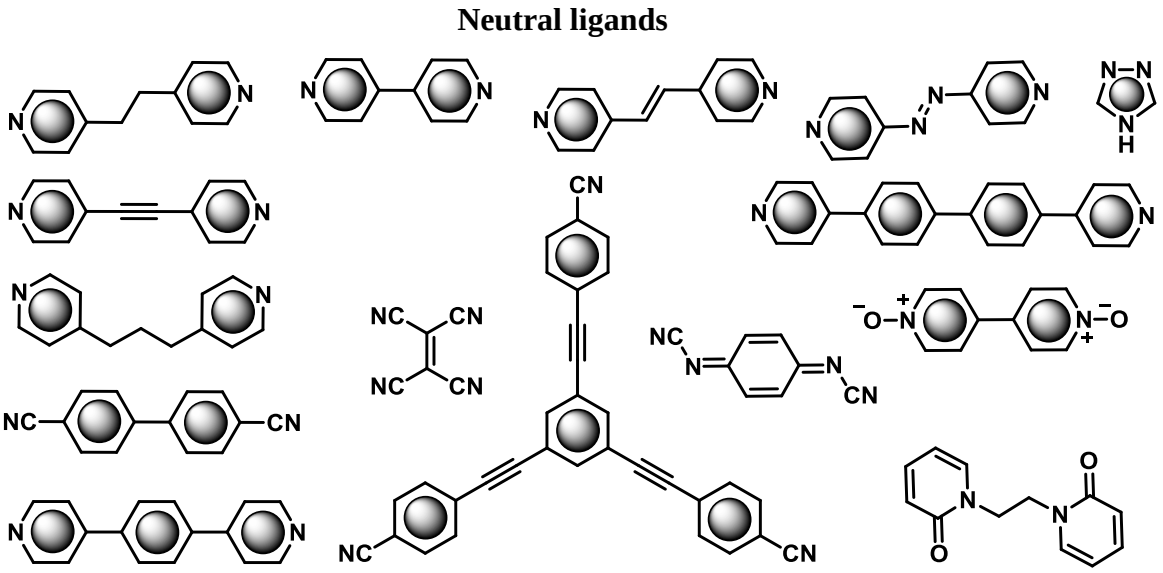

Figure 1.6 Neutral organic linkers used in the synthesis of coordintion polymers.

1.3.4 Motifs and Dimensionality

The self–assembly of molecular building blocks led to the coordination polymers of variant dimensionality (eg. one, two and three dimensional). Linearly organized organic ligands with two donor molecules (D), metal ions (M) and the spacer (S) are presented in black (Figure 1.7); here only coordination interactions are taken into account. Here dimensionality is regulated by the nodal centers (metal ions). One dimensional CPs are those in which metal ions are in coordination with two donor organic ligands in the infinitely arrayed polymeric chain; two dimensional CPs have metal ions in coordination with three or four organic ligands thus expanding the polymeric array in two directions; similarly three dimensional CPs can be constructed by metal ion coordinating to higher ligands.

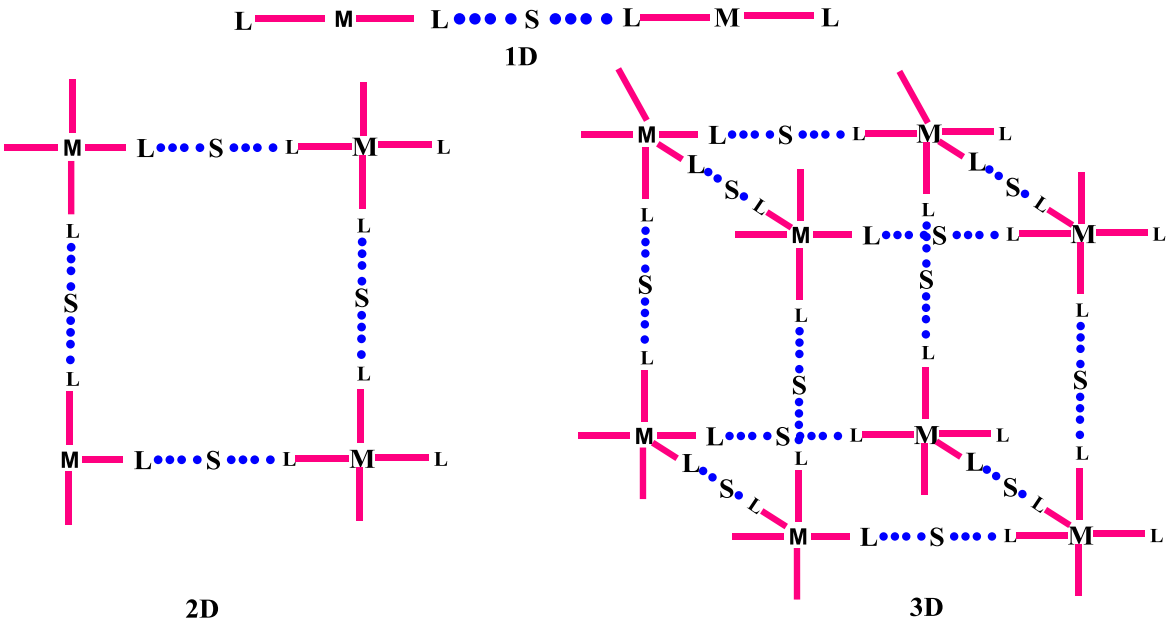

Figure 1.7 Coordination frameworks with various dimensionalities; here M–metal ions, S–spacer and L–linker [Janiak, 2003].

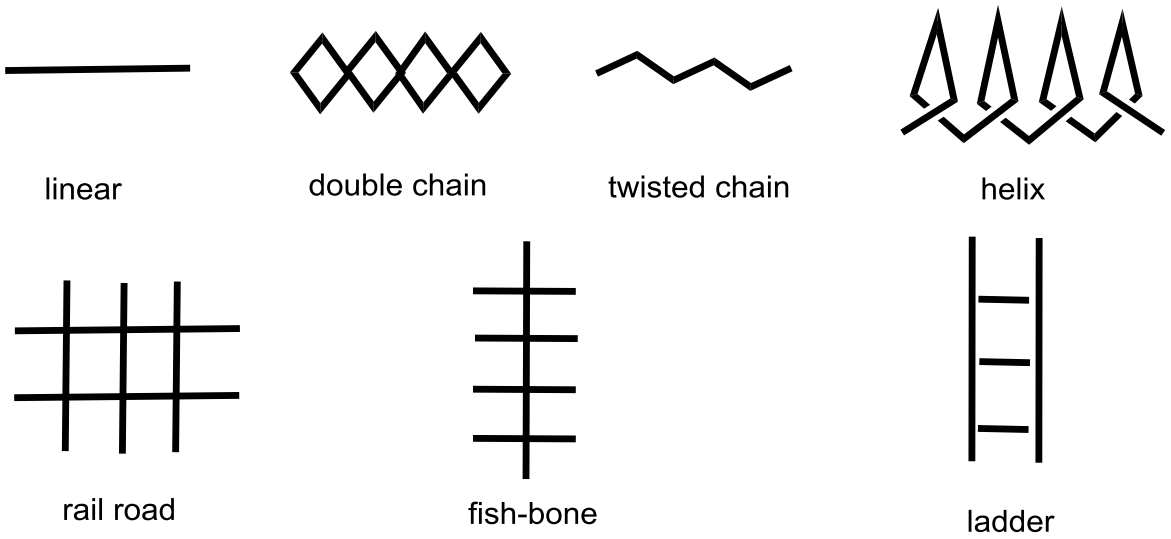

Figure 1.8 Possible shape of 1–D coordination framework.

The repeating units of coordination array have variations depending on the experimental conditions and elementary units of building blocks [Kitagawaand Noro, 2004]. The variation in the structure of coordination framework is represented using nodes and tectons and shown in figure 1.8. In view of various choices of elementary units, the versatility of the synthesized materials can be well explored. Some important examples of metal–organic frameworks will be shown in order to explore and overview the versatility of CPs and classify according to their dimensionality. The CPs primarly have the metal–ligand interactions, although there are several crucial interactions existing in the fabrication of these building blocks but the final dimensionality of CPs are only dependent on the metal coordination with ligands. We will explore only the systems with 2–mercapto–1,3,4–thiadiazole with gold and silver due to enormous abundance and importance of these systems.

1.4 One–Dimensional Coordination Polymers (1–D CPs)

The one–dimensional coordination polymer (1–D CP), the simplest topological coordination array, is found to be ubiquitous in nature and dominating in the field of coordination polymers.

The relative simplicity of the 1–D chains and their ease of formation allow us to incorporate interesting properties at the metal centers or in the backbone of the organic linkers much easily to develop strategies for engineering multifunctional polymeric materials. In the first review of coordination polymers published in 1964, Bailar discussed a few basic principles to synthesize coordination polymers along with various inorganic polymers based on cyano, hydroxo and halo bridging, which were mainly

characterized by non–crystallographic techniques [Bailar, 1964]. 1–D CPs are mainly associated with the linear chains in an infinite array. Some simple one dimensional CPs are represented in figure 1.9.

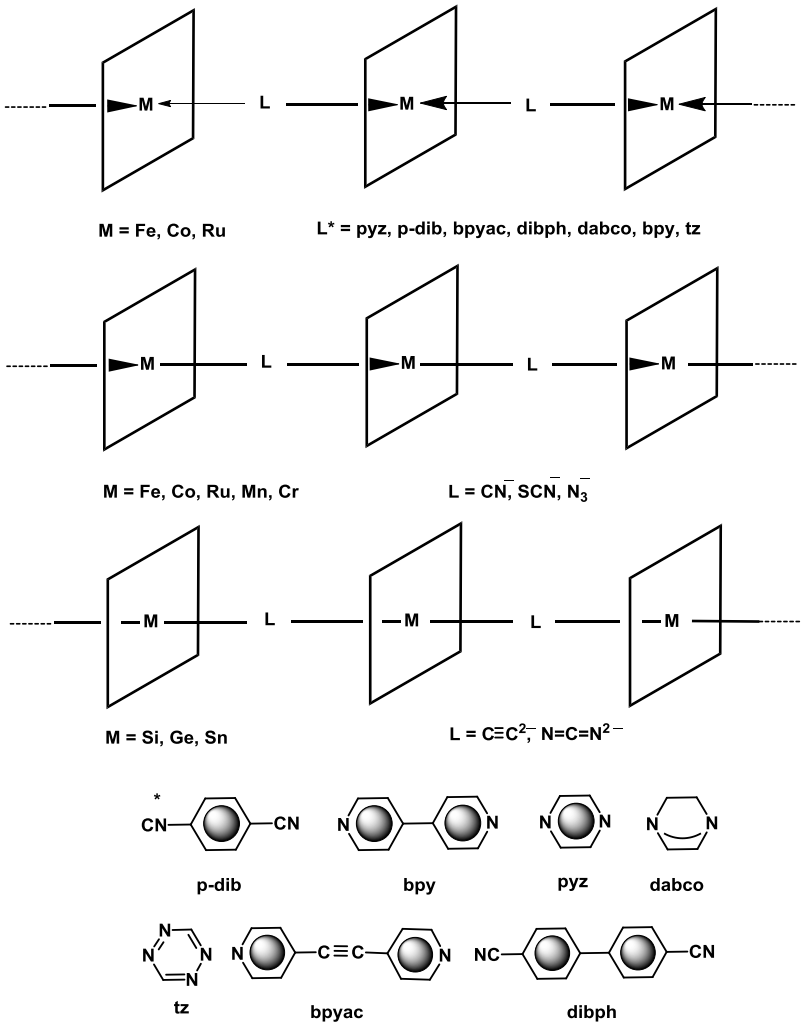

Figure 1.9 1–D coordination polymer networks.

1.5 Methods for the Synthesis of Coordination Polymers

There are four methods for the synthesis of coordination polymers reported in the literature [Kitagawa and Noro, 2004; Clegg, 2004]. However, it is essential to improve the synthetic methods for the advancement in architecture of coordination polymers. It is obvious that various procedures can be employed for the same starting materials but yielding different products since self–assembly occurs when the reagents are added together. Therefore molecular identification and sequentiality regulate the fabrication of pre–assumed products. The following processes are generally applied in order to grow single crystals of CPs. Mild conditions are required to grow single crystals, which can be obtained by sluggish evaporation of saturated solutions, rise in the temperature then controlled cooling causes variations in the solubility and results the appearance of crystals, the diffusion methods that are preferable to acquire single crystals suitable for X–ray analysis especially when the product is less soluble. The principle that regulates this process is to meet the available species very slowly. Next approach is a solvent liquid diffusion; in which various layers are assembled with a precipitating solvent and one product in suitable solvent, both in separate layers. The solvent moves into other layer and crystal grows at the interface of layers. Another method refers as the diffusion in solution, i.e. slow diffusion of reactants. This is quite familiar to the previous one, differing in the situation that here reactants are solubilized in both solutions with a physically separated solution layer. Although the hydro/solvo thermal techniques are frequently employed in the typical synthesis of zeolites, but used to design coordination polymers and explore the self–assembly in the products from soluble initiators. The operating temperature range is typically 120–250 ºC in an

autoclave under autogenous pressure. The lowered viscosity of water increases the diffusion process and thus favoring the possibility of crystal growth. The solubility difference between inorganic and organic components serves as a barrier in the construction of single crystals. This offers a non–equilibrium synthesis technique leading to metastable products. Alternate methods for the construction of coordination polymers are microwave and ultrasonic methods. The functioning of these techniques is based on the advancement of solubilities to react in a better way or crystallize the concerned products.

1.6 Significant Networks of Coordination Polymers

1.6.1 Ag(I) Coordination Polymers

The simple 1–D CPs of silver derived from N–donors are well–established and formed by two handed nodes with bipyridine based ligands [Blake et al., 1999; Khlobystov et al., 2001] although the CP of silver with 2,5–dimercapto–1,3,4–thiadiazole and 2–amino–5–mercapto–1,3,4–thiadiazole is still not explored. Generally, Ag(I) prefers the infinite arrayed linear geometry, although the coordination number of silver can vary from two to six all occurring due to its flexibility and structure from linear to octahedral. Furthermore, due to soft Lewis acidic nature and lack of ligand field stabilization effects, the geometry of Ag(I) coordination sphere gets deformed.

The tetrahedral and linear CP of silver are afforded by the linear 4,4'–bipyridine and silver salt depending on the proportion of silver and 4,4'–bipyridine ligand, in a ratio of 1:2 and 1:1 respectively; other geometry (T–shaped) can also be designed by

altering the reaction conditions of the same compounds [Yaghi and Li, 1996; Robinson and Zaworotko, 1995].

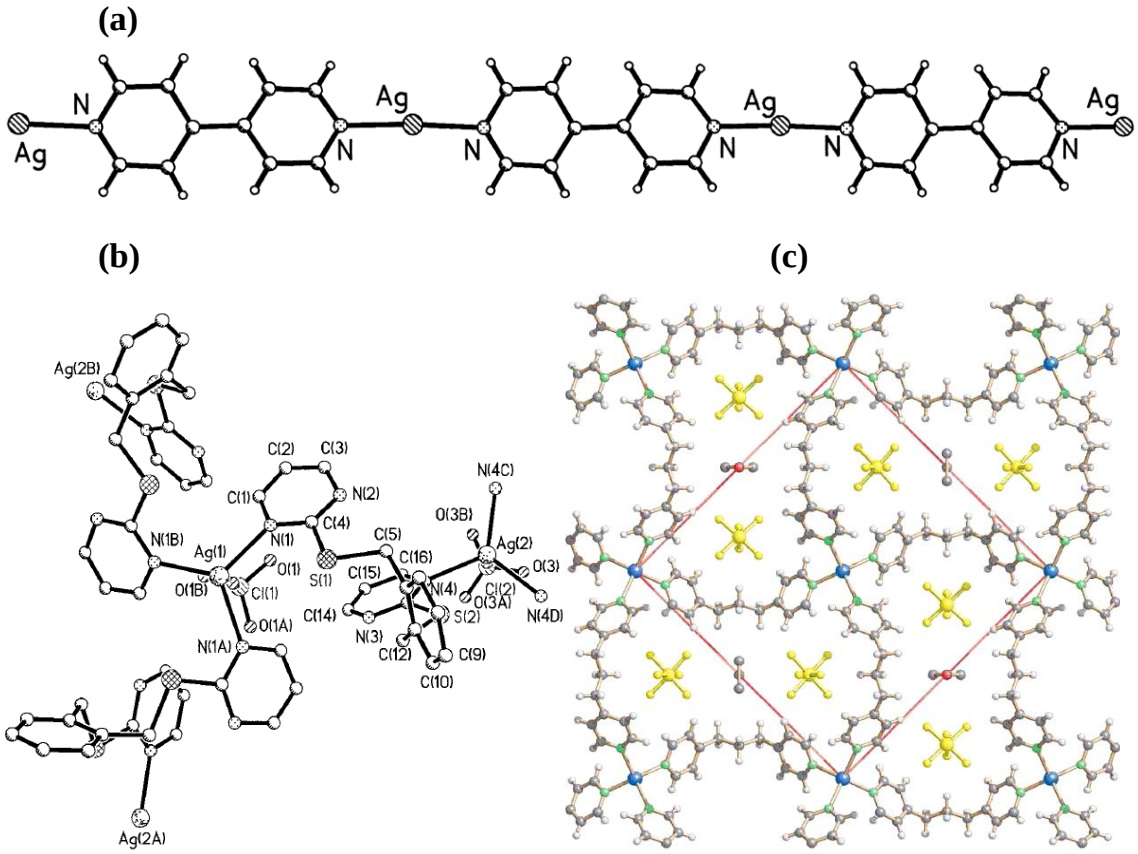

Figure 1.10 N–coordinated Ag(I); (a) [{Ag(4,4'–bipyridine)BF_4}$_n$] [Blake et al., 1999] (b) [{Ag_2(1,2–bis((2–pyrimidinyl)sulphanylmethyl)–benzene)$_3$}(ClO_4)$_2$]$_n$ [Hong et al., 2000] and (c) [{Ag(1,3–bis(4–pyridyl)propane)$_2$}SbF_6]$_n$ [Carlucci et al., 2002].

In the fabrication of silver coordination polymer, the number of coordinating N– and S– atoms are the major factor. Ag(I) is accommodated in various geometries with other linker bipyridine ligands; linear [Blake et al., 1999; Khlobystov et al., 2001] (Figure 1.10a), tetrahedral [Patra and Goldberg, 2002] (Figure 1.10c), and trigonal planar [Hong et al., 2000] (Figure 1.10b). Unlike the O–donor ligands, the N–donor

ligands do not favor the higher coordination number with the silver ions (Figure 1.11) [Ma et al., 2005]. The critical function of the weak interactions in the crystal construction is probed by flexibility of the silver ions. The bonds formed by the silver–donor atoms are significantly labile leading to the totally reversible complex formation.

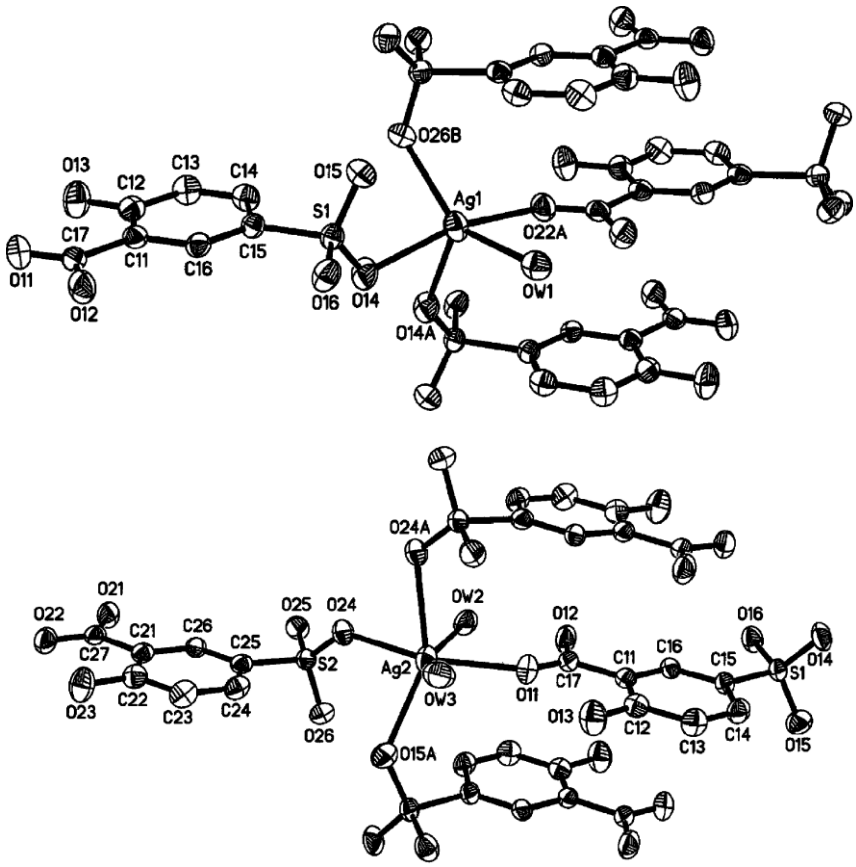

Figure 1.11 Silver attached with five and six donor atoms in $[\{Ag_2(HL)_2(H_2O)_3\}\cdot H_2O]_n$ (H_2L=5–Sulphosalicylic acid) [Ma et al., 2005].

1.6.2 Au(I) Coordination Polymers

Recently, it is possible to tailor the designed architectures of Au(I) with the organic ligands to deliver the desired building blocks followed by appropriate bridging. The assembly accommodates itself in molecular nature and they interact either through

π–π stacking or with the aurophilic interaction. The aurophilic interactions are weak interaction with the bond energy of 3–12 kcal mol^{-1} comparable to hydrogen bonding, the interaction is originated by the London forces [Hunks et al., 2000]. The coordination framework, Ph–C≡C–Au–C≡N–t–$Bu_2C_6H_2$–N≡C–Au–C≡C–Ph accommodates both aurophilic and π–π interactions (Figure 1.12). These CPs are highly stable since they comprise proficient crosslinking through aurophilic interactions and π–π stacking leading to the strong intermolecular association.

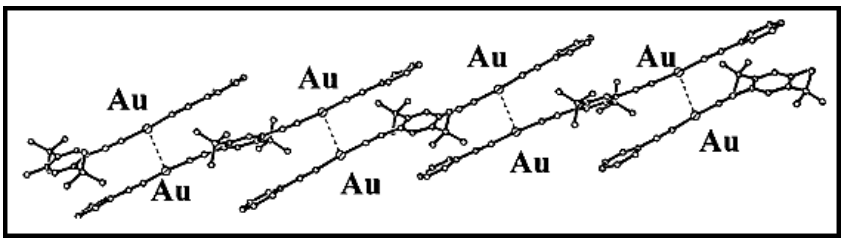

Figure 1.12 The aurophilic interaction in the solid state structure of [Ph–C≡C–Au–C≡N–*t*–$Bu_2C_6H_2$–N≡C–Au–C≡C–Ph] [Hunks et al., 2000].

Generally, Au(I) get linked with two alkynylorganic ligand in a linear array to design the anionic molecular species, $[RC{\equiv}C–Au–C{\equiv}CR]^-$ which is employed as a luminescent material. However, the only known cationic dialkynyl gold luminescent material $[MepyC{\equiv}C–Au–C{\equiv}CpyMe]^+$ is addressed by Ferrer et al. [Ferrer et al., 2003]. Irwin and coworkers developed $[–Au–C{\equiv}C–Ar–C{\equiv}C–Au–L–L–]_x$, where Ar = aryl and L–L=diphosphine or bis–(isocyanide). This coordination polymer has two bands appearing in the region 400–450 nm and 500–600 nm of emission spectra and are attributed due to metal perturbed ^{1}IL [π→π*(C≡C–R)] or ^{3}[π→π*(C≡C)]. The lower energy band is assigned due to ^{3}IL [π→π*] or ^{3}[σ→π*] or metal perturbed alkynyl ligand centred transition [Xiao et al., 1996; Irwin et al., 1997]. Interestingly, gold

coordination polymers with phosphine as counter ion exhibits $^{3}[\sigma(Au–P)\rightarrow\pi^{*}(C\equiv C)]$ transitions [Xiao et al., 1996; Irwin et al., 1997; Coco et al., 2008; Jia et al., 1993]. Gao and coworkers developed a series of phosphane– and (N–heterocyclic carbene)gold(I) coordination framework in which the longest wavelength emission, assigned due to arylacetylide ligand is oxygen–quenchable (origin triplet) and this transition is not observed in the parent ligand, which is indicative of the crucial role of Au(I) ion in the population of triplet state. The shorter wavelength transitions are attributed to the singlet fluorescence state [Gao et al., 2009]. Alkynyl gold coordination framework $[Au_3(Triphos)\{C\equiv CC_6H_4–p–(OCH_2CH_2)_2OMe\}_3]$ is designed to employ in molecular recognition. It shows turn on or off the fluorescence phenomenon of compound after the encapsulation of metal ions (Figure 1.13 and 1.14). Here, the emission and absorption phenomenon are changed once the metal ions are entrapped [He et al., 2009]. Yam et al. have designed di– and tetra– nuclear gold coordination polymers $[Au_4(dppm)_2(C\equiv C–L–C\equiv C)_2]$ and $[\{Au(PPh_3)\}_2(C\equiv C–L–C\equiv C)]$. It is a unique material employed for optical switches of gold alkynyl and azobenzene moiety (Figure 1.15) [Tang et al., 2007]. When the dichloromethane solution of both compounds are irradiated at 360 nm, [IL azo ($\pi\rightarrow\pi^{*}$)] transition induces a trans–to–cis photoisomerization, while the visible light irradiation into IL ($n\rightarrow\pi^{*}$) transition at 486 nm causes a cis–to–trans photoisomerization. This process is prohibited when alkynyl moieties are π–coordinated to Ag(I) centres, and further restored upon removal of Ag(I) coordinated ions *via* AgCl precipitation leading to the epilogue that photoswitching process can be modulated by Ag(I)–coordination/decoordination and thus illustrating a dual lockable input molecular photo logic switch (Figure 1.16).

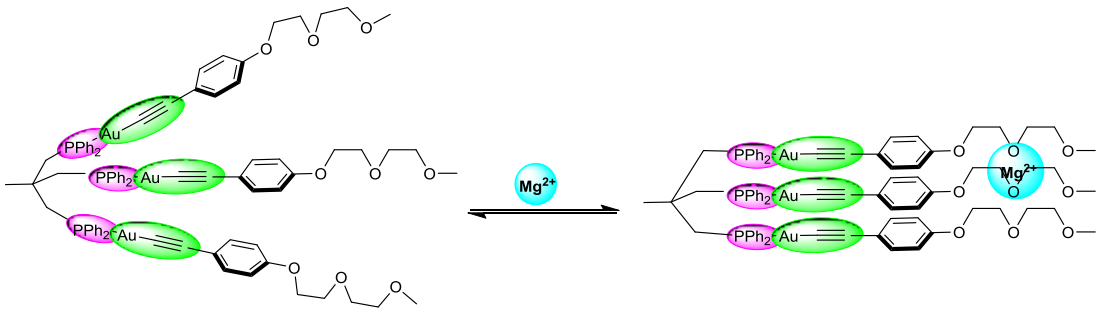

Figure 1.13 Schematic diagram of Mg^{2+} molecular recognition by $[Au_3(Triphos)\{C{\equiv}CC_6H_4{-}p{-}(OCH_2CH_2)_2OMe\}_3]$ coordination framework.

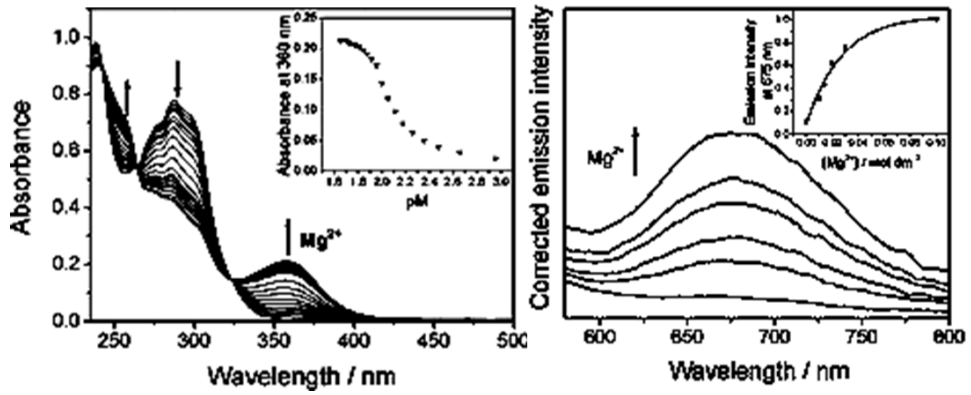

Figure 1.14 Fluorescence spectra of Mg^{2+} absorption by $[Au_3(Triphos)\{C{\equiv}CC_6H_4{-}p{-}(OCH_2CH_2)_2OMe\}_3]$ [He et al., 2009].

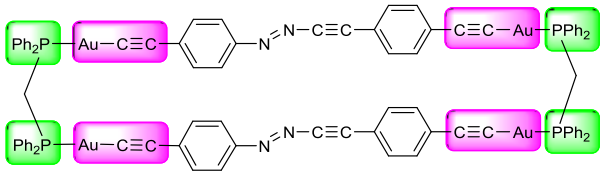

Figure 1.15 Supramolecular structures with phosphane–alkynyl–Au(I) entities.

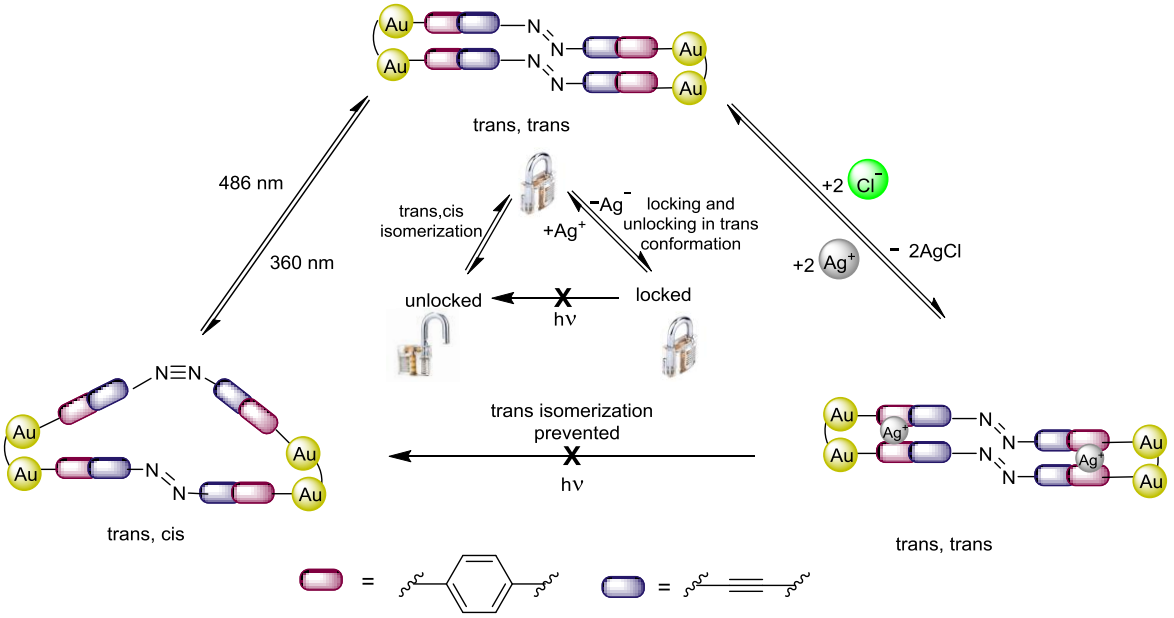

Figure 1.16 Photoswitching modulation mechanism facilitated by Ag(I).

1.7 Properties of Coordination Polymers

Coordination polymers are highly efficient sensors due to their high surface area and porous structure; also this high surface area with the presence of functional groups allow the coordination polymers to carry drugs proficiently and can be easily conjugated with active targeted ligands to further enhance drug accumulation in diseased locations and increase therapeutic efficacy. The coordination–assisted assembly strategy is expected to accelerate the development of new generation of photo–functional materials by rational tuning of optical properties of chromophores and proper selection of the metal species [Zhang et al., 2009]. Further the aqueous solutions of the coordination polymers of Ag(I) are reversibly transform from transparent to translucent states beyond certain temperatures. Subsequent investigations revealed that a fluorescence switching between the non–fluorescent and fluorescent stretched

compressed states of the supramolecular springs occur due to this dynamic conformational change. Such mechanical motions of the supramolecular spring offer a potential application in optical modulators, dynamic nano–devices and fluorescent thermometers [Kim et al., 2007]. Ultrasonic degradation of polymers is quite slow process but highly selective, and the scission rate is chain length dependent. In this view, a coordination polymer of silver(I) and N–heterocyclic carbene (NHC) ligand has an efficient ultrasonic scission and can be quantitatively cracked in minutes to provide highly reactive carbenes. Scission is irreversible in the presence of water. The mechano–chemical process that produce carbenes, catalyze organic transformations e.g. lactides polymerization and trans–esterification [Karthikeyan et al., 2008]. Their helical CPs display temperature regulated reversible extension–contraction motions. Further the aqueous solutions of the coordination polymers reversibly transform from transparent to translucent states above certain temperatures. Subsequent studies revealed that a fluorescence switching between the fluorescent stretched and nonfluorescent compressed states of the supramolecular helics occur due to this dynamic conformational change. Such mechanical motions of the supramolecular helical may be promising applications in the areas of dynamic nano devices, optical modulators, and fluorescent thermometers [Kim et al., 2007]. The coordination polymers can be employed as templates and sacrificial templates to engineer desired nanostructures [Moon et al., 2005]. CPs can be firstly prepared into nano form and then transformed to nano inorganic constituents. Here the morphology of the precursor is the deciding factor for the shape of the final materials.

1.8 Applications of Coordination Polymers

The growing interest in the fabrication of infinitely arrayed coordination polymers is due to the emergence of novel tunable functional materials. In this section, we will discuss how coordination polymers have potential and promising applications in the anion exchange and gas storage; caused by the porosity and zeolite like nature, luminescence/optical sensing, magnetism, catalysis and drug delivery.

1.8.1 Application to Gas–Storage and Gas–Separation

The coordination polymers depicting large pores and the pore size can be regulated by the appropriate ligand thus they can be efficiently used in the gas storage. The motif of copper, $\{[Cu(SiF_6)(4,4'–bpy)_2]\cdot 8H_2O\}_n$ with a robust 3–D channel exhibits efficiently high methane gas absorption along with the crystallinity and structure retention [Noro et al., 2000].

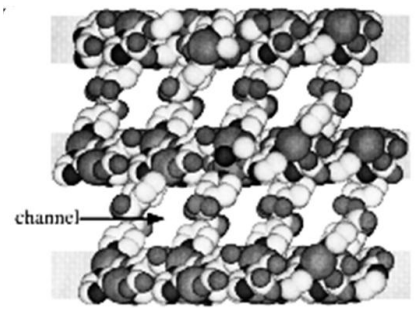

Figure 1.17 The channels, layers and pillers shown in 3–D structure of $\{[Cu_2(pzdc)_2(dpyg)]\cdot 8H_2O\}_n$ (H_2O is not shown here) [Noro et al., 2000].

A 3–D porous motif of copper formed by 2–D layer of $Cu_2(pzdc)_2$ and dpyg molecules (here pzdc = pyrazine–2,3–dicarboxylate, and dpyg = 1,2–dipyridylglycol) allows the easy removal of solvent and inclusion of specific guest molecule (Figure

1.17). It has the ability to remove the co–crystallized water molecules; further the X–ray diffraction analysis depicts the presence of two phases without guest molecules, the first one is anhydrous I that consist similar structure without water molecules and second one is apohost II with smaller inter–layer distances. It is established by the adsorption isotherm that second phase can selectively adsorb water and methanol but not carbon tetrachloride and at the end, final structure is same as the initial one. When the guest molecules are absent, the motif adjusts to avoid the extra space and the layers come closer.

Kitagawa et al. have reported CPs having capacity to change the structure, when contact with the guest–molecules and the pores adjust their shape to fit across the guest–molecules as shown diagrammatically (Figure 1.18) [Matsuda et al., 2004; Kubota et al., 2005]. These motifs have potential to finger print the target molecules. Consequently, Wright et al. have reported a series of third–generation motif of [Zn(bdc)] manipulated through the solid–state transformation and substitution by firmly hydrogen–bonded substances such as EtOH, MeOH, H_2O and DMF (Figure 1.19) [Edgar et al., 2001]. Herein, large structural modifications involve in these transformations. Furthermore, zeolites are frameworks of anionic building blocks and can only applicable for cationic exchanger while anions can be replaced frequently through these manupulated open motifs. It would be possible to build up anionic exchangers by utilizing the neutral ligand and cationic ion. Anion replacements are solid–state transformations and it occurs at the solid–liquid interface. Min et al. have reported motifs formed by silver salts and ethylenediamminetetrapropionitrile ligand

[Min and Suh, 2000] where, several anion replacements can be performed by immersing the crystals in suitable aq. solutions of $NaClO_4$, $NaNO_3$ and $LiCF_3SO_3$.

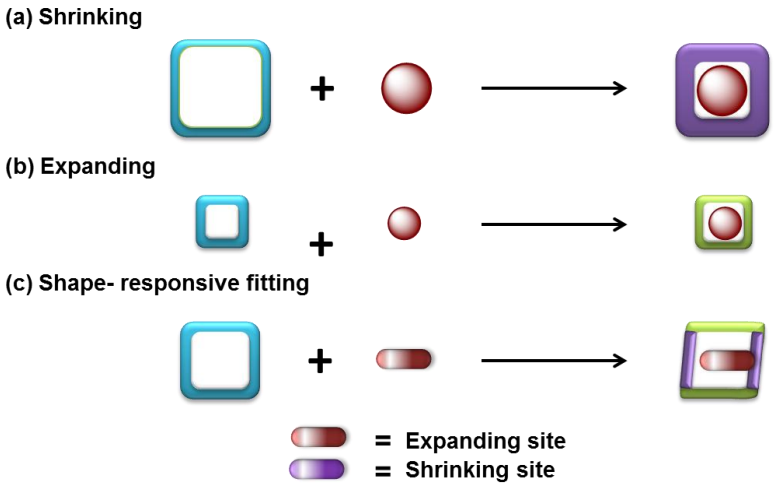

Figure 1.18 Diagramme for the adjustment of CPs.

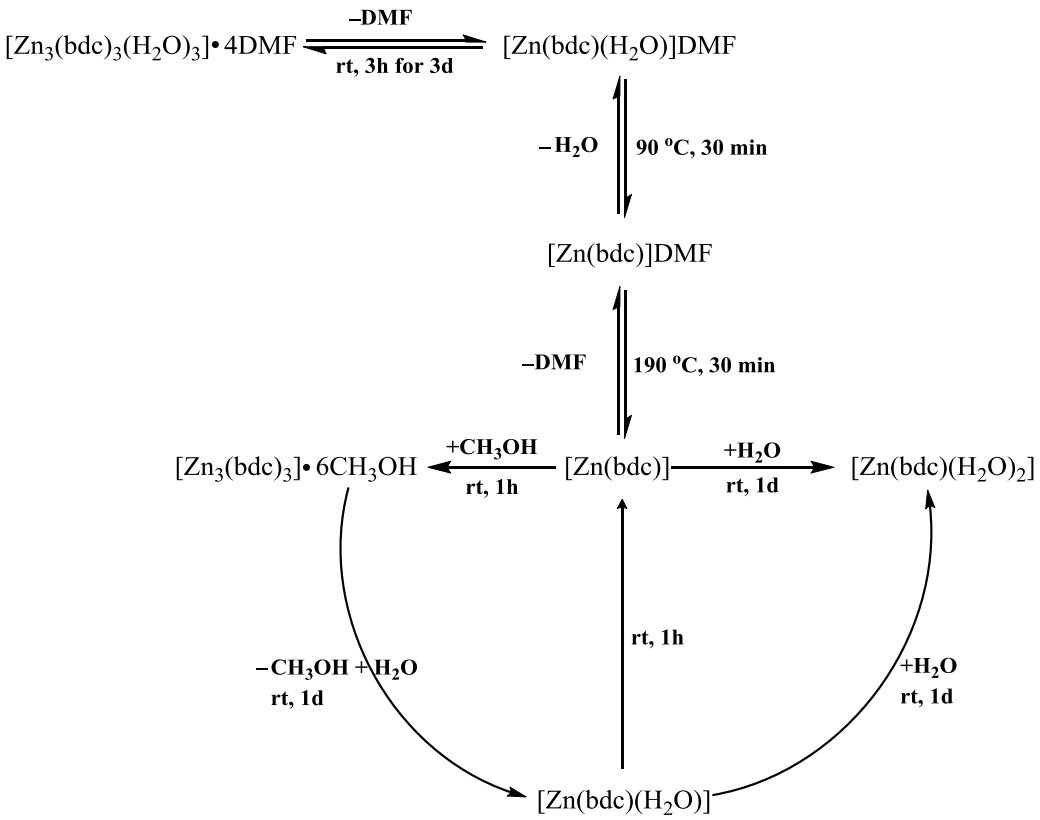

Figure 1.19 Summary of re–solvation and desolvation reaction in [Zn(bdc)].

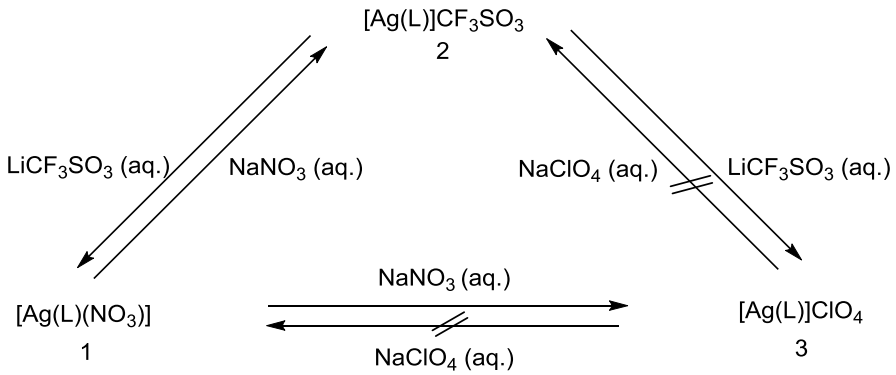

Figure 1.20 Anionic replacements of silver coordination framework by aq. solutions of $NaClO_4$, $NaNO_3$ and $LiCF_3SO_3$.

The triflate anions are reversibly replaced by nitrate anions (Figure 1.20), perchlorate anions; the nitrate substance alters the structure when replaced by perchlorate anions. It is necessary to mention that all these transformations occur in solid state followed by FT–IR and X–ray diffraction.

1.8.2 Application in Optical Sensing

The assembly of supramolecular building blocks has appealing interest in the luminescence due to their presence as the potential candidate in fluorescent sensors and optoelectronic devices. In fact, the organic–inorganic hybrid CPs can bear more stability related to solvent–, thermal–resistant rather than its classical colleague. Generally, the fluorescence measurements are performed in solid state at room temperature; however some solution phase measurements are also reported to establish the presence of oligomeric colleagues [Tong et al., 1999; Fei et al., 2001].

The phenomenon of ligand–to–metal charge transfer, caused by metal–ligand complexation can be precisely explained by emissions in the luminescence [Sun et al.,

2002; Fu et al., 2001]. These materials can be utilized to design light emitting diode devices due to their strong photoluminescence emission. There are two motifs, $\{[Tb_2(O_2CPh)_6(4,4'–bipyridine)]\}_n$ and $\{[Tb(O_2CPh)_3(CH_3OH)_2(H_2O)]\}$ with intense green emission, that exhibit spectral transition due to LMCT phenomenon (Figure 1.21). The emission spectra of ligand is not visible [Seward et al., 2001], thus the four bands appearing in the spectra is due to charge transfer from ligand to metal ions and correspond to the transitions $^5D_4 \rightarrow {}^7F_3$, $^5D_4 \rightarrow {}^7F_4$, $^5D_4 \rightarrow {}^7F_5$ and $^5D_4 \rightarrow {}^7F_6$.

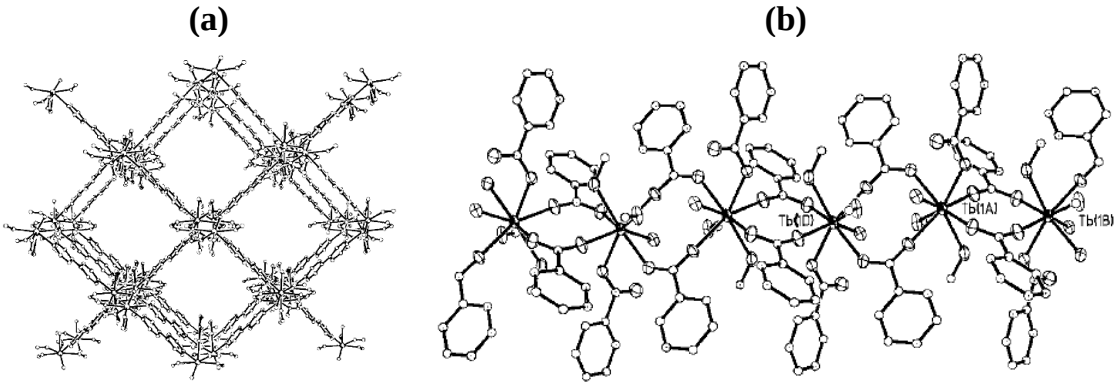

Figure 1.21 (a) 3–D structure of $[Tb_2(O_2CPh)_6(4,4'–bipyridine)]_n$; Benzoate molecules and Tb ions of 1–D chains are linked through bipyridine moiety, (b) 1–D chain in $[Tb(O_2CPh)_3(CH_3OH)_2(H_2O)]_n$; Tb ions are octa–coordinted with methanol, benzoates and water molecules [Seward et al., 2001].

Often the fluorescence intensity is increased efficiently in CP rather than the pure organic ligand without any alteration in the emission wavelength. The overall fluorescence phenomenon is credited due to organic ligand and the increment is arising due to enhancement in the ligand rigidity after complexation and thus resulting in decreased ligand symmetry. In some cases, blue, or red shift is noticed due to deprotonation of ligand or π–π stacking. For instance, the emission of terephthalate acid

appears at 466 nm whereas the $\{[Cd(terephthalate)(pyridine)]\}_n$ emits at 464 nm; although the emission of coordination polymer is caused by intra ligand (IL) π–π* transitions is almost 100 times higher than ligand itself [Fun et al., 1999; Liu and Xu, 2005]. Similarly $[Cu(PPh_3)(N,N–(2–pyridyl)(4–pyridylmethyl)amine)_{1.5}]\cdot 0.5CHCl_3\cdot ClO_4\}_n$ emits at 490 nm with 10 times larger intensity than the ligand itself, that shows emission at 460 nm. The observed red shift is caused by the probability of π–π stacking in the coordination polymer [Chen et al., 2000]. The room temperature luminescence property is quite uncommon in the motifs derived from silver; they are known to be low temperature luminescent materials with a significantly enhanced intensity with or without a slight shift in wavelength [Yeh et al., 2005; Dong et al., 2005]. The origin of luminescence property in the coordination polymer containing Ag–Ag contacts may be due to scant metal–metal contacts. The argentophilic interaction is only observed in $\{[Ag(4–PDS)]OTs\}_n$ derived from 4,4'–dipyridylsulphide (4–PDS) and AgX (where X=NO_3^-, ClO_4^-, PF_6^-, BF_4^-, and OTs^-); consequently the fluorescene phenomenon noticed in this framework is corresponding to the band at 600 nm for Ag–Ag interactions [Horikoshi et al., 2000].

1.8.3 Application as Magnetic Materials

Another interesting application of CPs is observed as promising magnets. Actually, ferrimagnetism, anti–ferromagnetism and ferromagnetism are the conjunctive processes of the magnetic spins expecting coupling or interaction between the paramagnetic spin centers and the building blocks of CPs. This building block regulates the selection of coupling parameters. The essential condition for the magnetic CPs is to

have a permanent residual magnetization in the absence of field for a high possible critical temperature and to provide a parallel (ferromagnetism) or non–equal anti–parallel (ferrimagnetism) coupling of neighboring spins carriers leading to a bulk compound with a non–zero spin. Several examples of antiparallel coupled spins (anti–ferromagnetism) also exist since high–spin multiplicity is often less stable than the lower counter parts.

The efficient magnetic coupling in CPs occurs *via* open shell ligands. Cyano, oxo or azido linkers explore intense coupling through unpaired electrons and metal centers. For instance, Batten et al. have reported a review that lightens the interlinking between magnetic properties and structures of CPs with tricyanomethanide and dicyanamide groups [Batten et al., 2003]. The CPs containing carboxylate ligands have remarkably intense magnetic behavior. Some 2–D motifs constituting mixed metals such as Mn(II), Fe(II) or Cu(II) display ferromagnetism due to the 1–D repeating unit (–M–O–C–O–Cu–O–C–O–M–) [Noro et al., 2005] (Figure 1.22). Several metal–carboxylate CPs are developed by using the ligands that reinforce the intense coupling and framework stability. Zaworotko et al. developed the room temperature ferromagnetic coordination polymer of Cu, $[(Cu_2(pyridine)_2(bdc)_2)_3]_n$ [Moulton et al., 2002]. However, there are rare examples for the magnetic CPs derived from nitrogen based polytopic ligands. For instance, $\{[Fe_2(trans–4,4'–azopyridine)_4(NCS)_4]\cdot EtOH\}_n$ displays magnetic moments depending on temperature variation originated by spin–crossover nature [Halder et al., 2002]. The ligands with larger length reduces the coupling possibility in metal centers, e.g. $\{[Co(L)_2(NCS)_2]\cdot[H_2O]_{2.5}\}_n$ (here L = 2,5–bis(4–pyridyl)–1,3,4–thiadiazole) and $\{[Cu(L)(H_2O)(SO_4)]\cdot 2H_2O\}_n$ display weak

antiferromagnetic coupling [Huang et al., 2004]. Some other examples are also studied with co–ligands of carboxylic and *N,N'*–donors [Manson et al., 2005]; where the carboxylic linkers are employed as pillars in metal–*N*–*N'*–donor ligands providing the essential coupling.

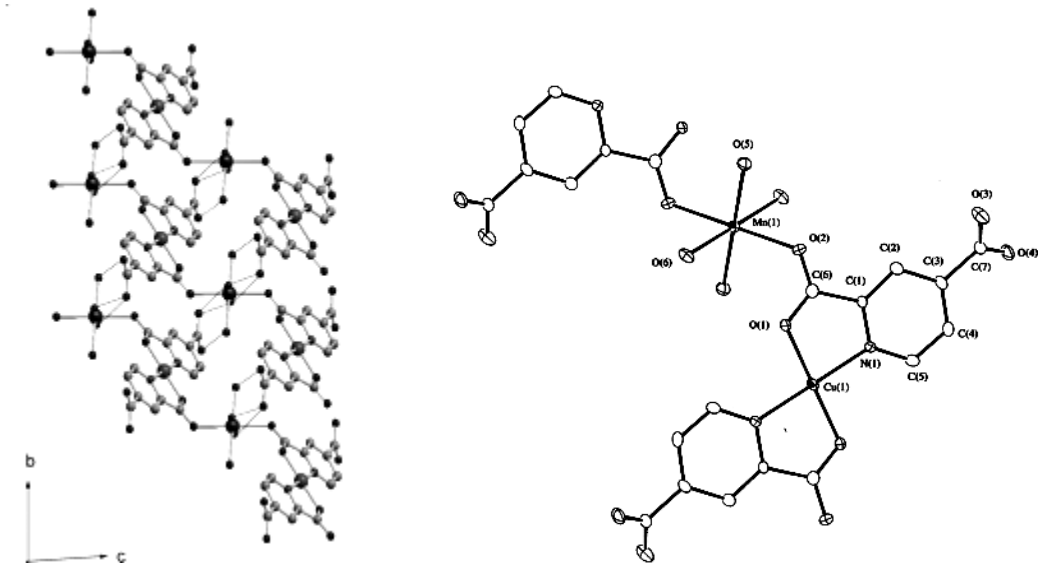

Figure 1.22 Coordination network of $[Mn\{Cu(pyridine–2,4–dicarboxylate)\}_4(H_2O)_4]_n$ [Noro et al., 2005].

The spontaneous ordering of anti–ferromagnetism in $\{[M(oxalate)(4,4'–bipyridine)]\}_n$ (here M=Co^{2+}, Fe^{2+} or Ni^{2+}) is attributed due to the intense exchange interactions in 1–D bridged metal ions *via* interchain magnetic interactions and oxalate ligands [Yuen et al., 2000].

There are various examples of CPs containing mixed ligands that can intimately demonstrate the magnetism in CPs [Wen et al., 2005]. The Cu(II) ions exhibit poor anti–ferromagnetism through the azide bridge in $\{[Cu(N_3)_2((1R)–6,6–dimethyl–5,7–methano–2–(2–pyridinyl)–4,5,6,7–tetrahydroquinoline)]\}_n$.

1.8.4 Application in Shape/Size Selective Catalysis

CPs can act as efficient catalysts since they are porous in nature and have active metal centers; also they can be engineered to provide specific organic ligands and metal centers. Interestingly, several non–porous CPs also act as promising catalysts. Additionally, coordination polymers are the potential candidate for heterogeneous catalysis in their solid form; since the major drawback in the liquid state heterogeneous catalysis is their short range stability. The catalytic cycle should progress without degradation or dissolution so that the ligand wouldn't react with the metal centers and vice–versa; that's why there are a few reports in the literature for effective catalysis with these materials. Aoyama et al. have reported CPs formed by anthracenebisresorcinol (H_4L) (Figure 1.23) and $Ti(O^iPr)_2Cl_2$, $Al(CH_3)_3$, $La(O^iPr)_3$ or $Zr(O^tBu)_4$, that exhibit effective catalysis [Dewa et al., 2001; Sawaki and Aoyama, 1999]. For illustration, a microporous motif of $\{[Zr_2(L)(O^tBu)_2]\}_n$ have unknown structure due to insolubility in all common organic solvent, and can serve as reversible guest acceptor for benzene, hexane, ethylacetate; and as efficient selective catalyst in Diels–Alder reactions without any contamination (Figure 1.24).

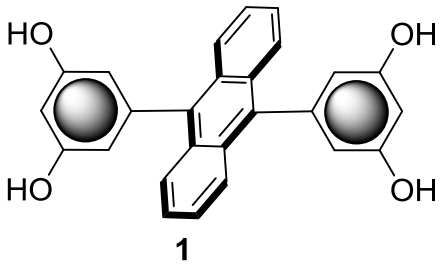

Figure 1.23 Anthracenebisresorcinol (H_4L).

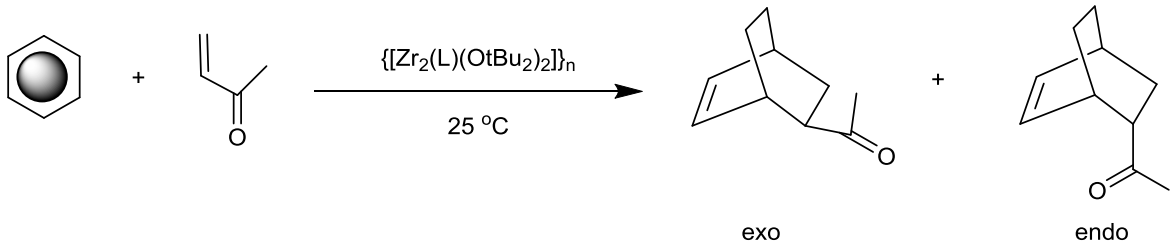

Figure 1.24 Catalytic activity of $\{[Zr_2(L)(O^tBu)_2]\}_n$ in Diels–Alder reaction.

Now–a–days, a number of coordination polymers are developed that are suitable in asymmetric heterogeneous catalysis [Dai, 2004]. The specific purpose to choose these materials is to allow the pores with chiral environment to regulate the enantio–selectivity and the metal ions as a catalytic center. For instance, Sasai et al. have developed chiral motifs assembled through 1,1'–2,2'–binaphtol based chiral ligand (Figure 1.25) and Ti(II), Al(III) ions. They are extremely insoluble in commanly used organic solvents. The motif, $\{[Ti_2(\mu\text{–}O)_2(binol)]\}_n$ catalyses the asymmetric carbonyl–ene reaction (Figure 1.26) and the product of the reaction was related to the classical homogeneous catalysis.

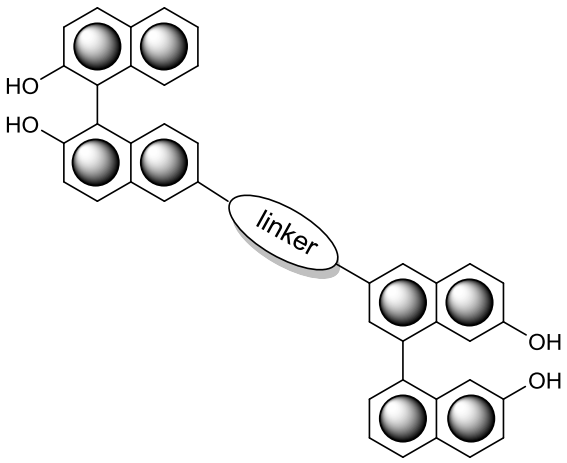

Figure 1.25 Structure of 1,1'–2,2'–binaphtol based ligand.

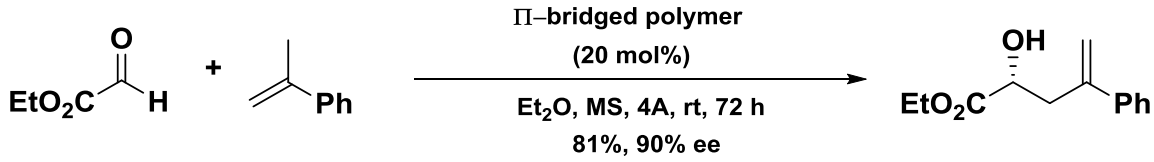

Equation 1.26 Catalytic activity of $\{[Ti_2(\mu\text{–}O)_2(binol)]\}_n$ in asymmetric carbonyl–ene reaction.

1.8.5 Application in Drug Delivery

In recent years, scientists have explored the application of coordination polymers in drug delivery. The great potential of using coordination polymers as drug delivery systems largely relies on these factors: (1) porosity and high surface area [Sawaki et al., 1998]; (2) low toxicities of certain metals, i.e. Fe, and Zn etc. (3) significant chemical and physical stabilities [Dai, 2004; Takizawa et al., 2003]; and (4) well–defined chemical compositions. In 2006, Ferey et al. have first reported the proof of coordination polymers in drug delivery [Du et al., 2002]. Two mesoporous coordination polymers, chromium–based MIL–100 and MIL–101 (MIL, Materials of Institut Lavoisier) [Lor et al., 2002] were chosen as drug carriers for Ibuprofen (IBU). The X–ray powder diffractions (XRPD) of both materials established that their frameworks are retained even after drug loading. The N_2 adsorption after the drug adsorption experiments indicates the absence of residual porosity. Both materials depicted significant drug loadings: MIL–100 with 35% (w/w) of Ibuprofen/ carrier and MIL–101 with 140% (w/w) of Ibuprofen/carrier. In another investigation by Ferey et al., they have reported flexible coordination polymers as drug delivery systems [Sun et al., 2002]. The work concerned with two porous coordination polymers; MIL–53(Cr) and MIL–53(Fe) [Rao et al., 2000], revealed flexibile drug loading ability upon the

adsorption of guest molecules. Both MIL–53 materials could adsorb upto 20% w/w of Ibuprofen/carrier. Rosi et al. have reported experiments that deal with cation–triggered drug release from a zinc–adeninate coordination polymer [Zhao et al., 2001]. In this report, the coordination polymer $[Zn_8(ad)_4(BPDC)_6O{\cdot}2Me_2NH_2{\cdot}8DMF{\cdot}11H_2O]_n$ (ad = adeninate; BPDC = biphenyldicarboxylate), referred as bio–MOF–1, and successfully used as the drug carrier. The ligand adenine was chosen for its remarkable coordination capacity and biocompatibility. Drug loading of procainamide·HCl into bio–MOF–1 was performed by multi–steps of cation exchange experiments. Bio–MOF–1 could achieve 22% (w/w) of drug loading (procainamide·HCl/carrier), comparable to MIL–53. Here, more than 70% of drug was released within 20 h and complete release was realized in 3 days. However, only 20% of procainamide was released in a comparative experiment of bio–MOF–1 in deionized water.

1.9 Ligands: Important to Tune the Structure of Coordination Polymers

The ligands have to bridge between the metal ions in the fabrication of coordination polymers. Therefore it must be multi–dentate with two or more donor atoms. These bridging ligands are termed as di–, tri–, tetra–topic depending on the number of donor atoms. The diversity of organic components is, of course the basis for the variety in structural topologies [Moulton and Zaworotko, 2001]. Thus by appropriate selection of organic ligands, one can tune the physical and chemical properties of designed coordination polymers and thus can be employed for enormous applications, e.g. electrical conductivity, catalysis, magnetism, luminescence, zeolitic behavior and non–linear optics. Generally, sulphur, nitrogen– and oxygen– donor

ligands particularly feature prominently in the fabrication of coordination polymers [Munakata et al., 1999; Oxtoby et al., 2002]. The thiol and amino derivatives of 2–mercapto–1,3,4–thiadiazole based organic ligand are the prominent example for a prototypical bridging ligand. These are interesting molecular building blocks since they can effectively form diverse architectures with the metal connectors. These ligands offer two different donor sulphur sites located at their terminals. These sulphur donor atoms differ in steric requirements and basic character. Thus the endocyclic sulphur atom is a weaker donor than the exocyclic one. Definitely this is also due to the geometrically and symmetrically feasible coordination with exocyclic sulphur atoms. Therefore the selection of appropriate ligands play crucial role in the self assembly and organization of developed coordination network.

1.9.1 2–Mercapto–1,3,4–thaizoles: An Eminent Class of Lignads

Generally multidentate organic ligands are preferred as tectons for the polymerization of metal ions into an extended array of network, since these organic ligands offer several coordination modes and facilitate the fabrication of multi–dimensional coordination polymers [Biradha et al., 2010; Walker et al., 2004; Yaghi et al., 2003; Chen et al., 2008]. In this aspect, 2–mercapto–1,3,4–thiadiazole based organic ligands (2,5–dimercapto–1,3,4–thiadiazole and 2–amino–5–mercapto–1,3,4–thiadiazole) are particularly significant since firstly they can protonate partially or completely to generate dianions which make the coordination significantly feasible and secondly the geometry of the ligand which allows the various metal ion coordination geometrically and symmetrically feasible. Thirdly the aromatic rings of organic ligand provide stability to the developed coordination network *via* π–π stacking and hydrogen

bonding. Further, very few reports are available about the coordination chemistry of DMTD and AMT, which indicate that it is imperative to attain more insights into DMTD and AMT as ligands to fabricate the multidimensional coordination polymers [Biradha et al., 2010; Vasimalai and John, 2012]. Furthermore, the introduction of sulphur and nitrogen containing organic ligands in the chemical reactions may yield several novel coordination frameworks with interesting morphology and promising functionality. In addition to that, sulphur and nitrogen containing rigid rod like bifunctional organic ligand can be applied to fabricate infinite arrayed 1–D polymeric networks thereby providing feasibility to the assembly of coordination polymers. Moreover, sulphur and nitrogen containing aromatic ligands can orient the ring to facilitate the low dimensional array to extend into multidimensional one [Fe´rey et al., 2005; Roesky and M. Andruh, 2003].

1.9.2 Structrual Features of 2–Mercapto–1,3,4–thiadiazole Ligand

Advantage of 2–mercapto–1,3,4–thiadiazole derivatives is their natural framework with rich functional groups, offering intriguing topologies when inserted as building blocks in supramolecular hierarchical self–assemblies. Moreover in terms of cost, availability and bio–compatibility these are considered to be an appriproate choice (Behave like adeninate based MOFs). Despite these vast benefits, comparatively less work has been reported for coordination frameworks originated from 2–mercapto–1,3,4–thiadiazole derivatives. The amine and thiol moiety present at both terminals may act as bridging group that is highly desirable in the construction of functional porous and crystalline network of coordination polymers. Advantage of such systems is the existence of diverse set of coordinating groups on the same ligand backbone: i.e., thiol,

amine and azo group. Furthermore, the heterocyclic aromatic ring is capable of forming infinite arrayed architectures through the π–π interactions and hydrogen bonding, thus leading to the controlled and regular network. It is obvious that, by increasing the ability of the ligand to form π–π interactions, the construction of longer–range coordination polymer networks is faciliated.

1.10 Nano–Coordination Polymers

Recent two decades have addressed and evidenced the rapid innovations and development in nanotechnology and efficient reports have been dedicated to explore the clinical use of this nano–research for the diagnosis, detection and treatment of several severe diseases (Lin, et al., 2009). These nanostructures have promising application in biomedical areas due to tailorable surface chemistry, controllable drug release kinetics, enhanced permeability, high matrix loading, enhanced biocompatibility, improved tumor accumulation, active tumor targeting and retention effect [Peer et al., 2007; Daniel and Astruc, 2004; Kim et al., 2009]. The controlled and directed design of metal–organic coordination nanostructures is an emerging area of growing interest (Taylor–Pashow et al., 2010). Beyond the designing of molecular nano–architectures with uniform, well–defined sizes and morphologies is required in a number of emerging areas, e.g. nanomedicine, [Novio et al., 2013; Horcajada et al., 2010] where exact controll over nano–scale dimensions are essential for the internalization of functional materials into molecular electronics [Imaz et al., 2008] or cells; [Novio et al., 2014] where each structure represent a bit of information. Further, miniaturization can also increase colloidal dispersion, improve the surface area and the sensing, catalytic and storage abilities.

1.10.1 Diversity in the Domain of Nano–Coordination Polymers

Nanostructured materials have aroused worldwide and appealing interest as they often explore novel and interesting size–dependent chemical and physical properties [Batten and Robson, 1998; Eddaoudi et al., 2002]. By scaling the coordination polymeric framework up to the nanometer scale, the scope of metal–organic materials will be broaden and lead to an interesting class of highly tailorable nano–scale coordination polymers (NCPs) that illustrate the application of this interesting class in various fields, ranging from catalysis, sensing and drug delivery; and prompt their implementation in the remarkably effective imaging techniques, e.g. positron emission tomography (PET), optical imaging, computed tomography and magnetic resonance imaging [Horcajada et al., 2009]. There is a vast variation in the domain of nano–sized coordination polymers and herein, we are confining the discussion to nanostructured crystalline, amorphous and porous coordination polymers. This thesis highlights the synthesis and effective use of nano–structured assembly of coordination polymers in quantitative assay of life saving drugs. The functionality of nano–assembly exhibit high sensitivity and selectivity for the sensing of drugs as the nano–belts are π–rich structures which can strongly bind with the specific drug molecules through the π–π interactions and the effective electron channeling occurs through the nanopore channels, thus providing highly sensitive and ultra level detection of drugs. Nano coordination polymers have been now playing an important position in the era of porous/crystalline materials and distinguished as a special category in the conventional classification of materials.

1.10.2 Nano–Porous Coordination Polymers

The area of porous coordination polymers (PCPs) has appealling attention in the last few years. Every year the number of reports dealing with porous coordination polymers is constantly increasing. Several groups have focused on the development of new porous coordination polymers using the limitless permutations of metal cations and organic linkers [Yaghi et al., 2003; Kitagawa et al., 2004]. Significant effort has been dedicated to design a variety of nano–scale materials. These are rationally designed by modifying organic ligands and varying coordination geometries. Therefore, these prominent features assist to precisely design the pore sizes, channel structures and pore and surface functionalities [Eddaoudi et al., 2002; Horike et al., 2009]. The inherent properties of PCPs are basically dominated by the framework topology, pore size, chemical structures and pore surface functionality. In this context, significant efforts have been dedicated to the synthesis of novel materials and evaluate their molecular–based properties at the early stage of this research field. Furthermore, the nano–scale structure is one of crucial factors to sophisticate the properties, especially for catalytic activity, separation, adsorption kinetics and efficiency [Aguado et al., 2011; Kitaura et al., 2002]. Moreover, the morphology and size of PCPs intensely influenced the critical properties of coordination framework. Due to their high specific area, chemical tenability and porosity, these are promising materials for application in heterogeneous catalysis, biomedical imaging, drug delivery and sensing.

1.10.3 Interesting Nano–Coordination Polymer Networks

Considerable effort has been devoted to the design of nanoscale coordination polymers in last few years. For instance, Lin’s et al. have prepared nano rods of

$[Ln_2(BDC)_3(H_2O)]$ in CTAB/*iso*–octane/1–hexanol/water reverse emulsion system (CTAB = cetlytrimethylammonium bromide, Ln = Gd^{3+}, Eu^{3+} or Tb^{3+}). The morphology of particle was dependent on water to surfactant molar ratio of emulsion (*w*). For instance, *w* value of 5 provide $[Gd_2(BDC)_3(H_2O)]$ nano–rods with length and diameter of 100–125 nm and 40 nm respectively (Figure 1.27a). When *w* value increases to 10, nano–rod length changes up to 1–2 μm length and ~100 nm diameters [Rieter et al., 2006, 2007, 19,20]. Furthermore, nano–plates of [Gd(1,2,4–BTC)$(H_2O)_3$(1,2,4–BTC = 1,2,4–benzenetricarboxylate) (Figure 1.27c), nano–rods of $[Mn(BDC)(H_2O)_2]$ (Figure 1.27d) and $[Mn_3(BTC)(H_2O)]$ (Figure 1.27e and f) were designed *via* reverse emulsion method [Rieter et al., 2006; Taylor et al., 2008]. Gref and coworkers synthesized several nano coordination frameworks of Fe(III) with a series of multifunctional ligands H_3BTC, H_2BDC and fumaric acid etc. in various solvents at temperature higher than 100 ºC (Figure 1.28a–c) [Horcajada et al., 2010]. Bai et al. synthesized nano–porous cube of MOF–5 by diluting the reactants *via* solvo–thermal conditions (Figure 1.28d) [Xin et al., 2010]. They developed the hierarchical Cr–BDC and meso–porous Cu–BDC nanoparticles *via* solvo–thermal reactions [Xin et al., 2010]. Zhong and coworkers developed infinite coordination polymer hollow microspheres of rare earth–based 4,4′,4″–benzene–1,3,5–triyl–tri–benzonate (RE–BTB) *via* a mixed solvothermal route (Figure 1.28e and f) [Zhong et al., 2011]. In addition to that Lin et al. prepared $[Gd_2(BHC)(H_2O)_6]$ (BHC = benzenehexacarboxylate) nanoparticles using the microemulsion–assisted solvo–thermal synthesis at 120 °C for 18 h [Taylor et al., 2008]. Kitagawa and coworkers have efficiently contributed in the area of porous coordination polymers. They synthesized $[Cu_3(BTC)_2]$ crystals by microwave

assisted coordination modulation. The size of $[Cu_3(BTC)_2]$ crystals can be regulated, varying from few tenths of nanometer to micrometers, by adjusting the concentration of dodecanoic acid and the ratio between dodecanoic acid and H_3BTC (Figure 1.29) [Diring et al., 2010]. Jhung and coworkers synthesized nano–sized MIL–101, with huge porosity in various conditions of pH, synthetic techniques and concentrations [Khan et al., 2011]. Lin and coworkers showed that nanoparticles of $Fe_3(\mu_3–O)Cl(H_2O)_2(BDC)_3$ can be prepared by microwave irradiation at 120 ºC [Pashow et al., 2009].

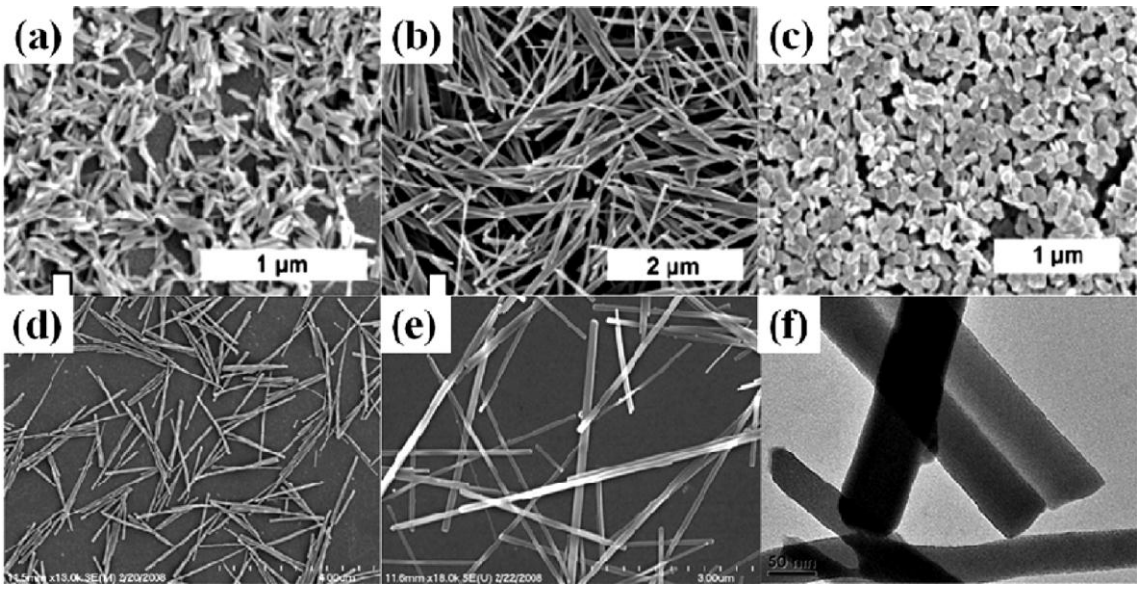

Figure 1.27 SEM micrograph of $[Gd_2(BDC)_3(H_2O)]$ nanorods designed with w = 5 (a) and w = 10 (b), $[Gd(1,2,4–BTC)(H_2O)_3]$ nano–plates (c), [Rieter et al., 2006], $[Mn(BDC)(H_2O)]$ nano–rods (d), $[Mn_3(BTC)_2(H_2O)_6]$ (e), and TEM micrograph of $[Mn_3(BTC)(H_2O)_6]$ nano–rods (f) [Taylor et al., 2008].

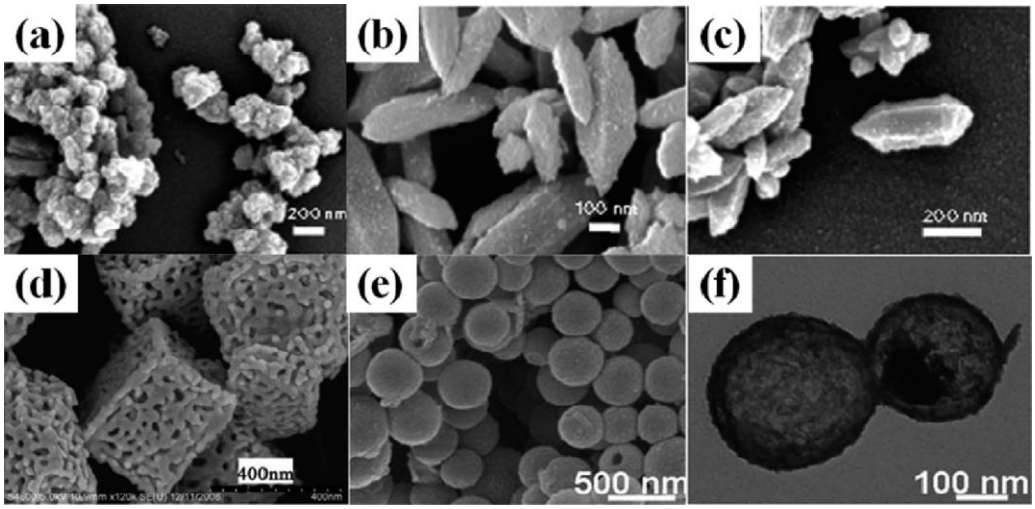

Figure 1.28 SEM micrograph of MIL–100 (a), MIL–88A (b), PEGylated MIL–88A nanoparticle (c), [Horcajada et al., 2010] nanoporous cube of MOF–5 (d) [Xin et al., 2010], RE–BTB hollow microspheres (e) and TEM micrograph of RE–BTB hollow spheres (f) [Zhong et al., 2011].

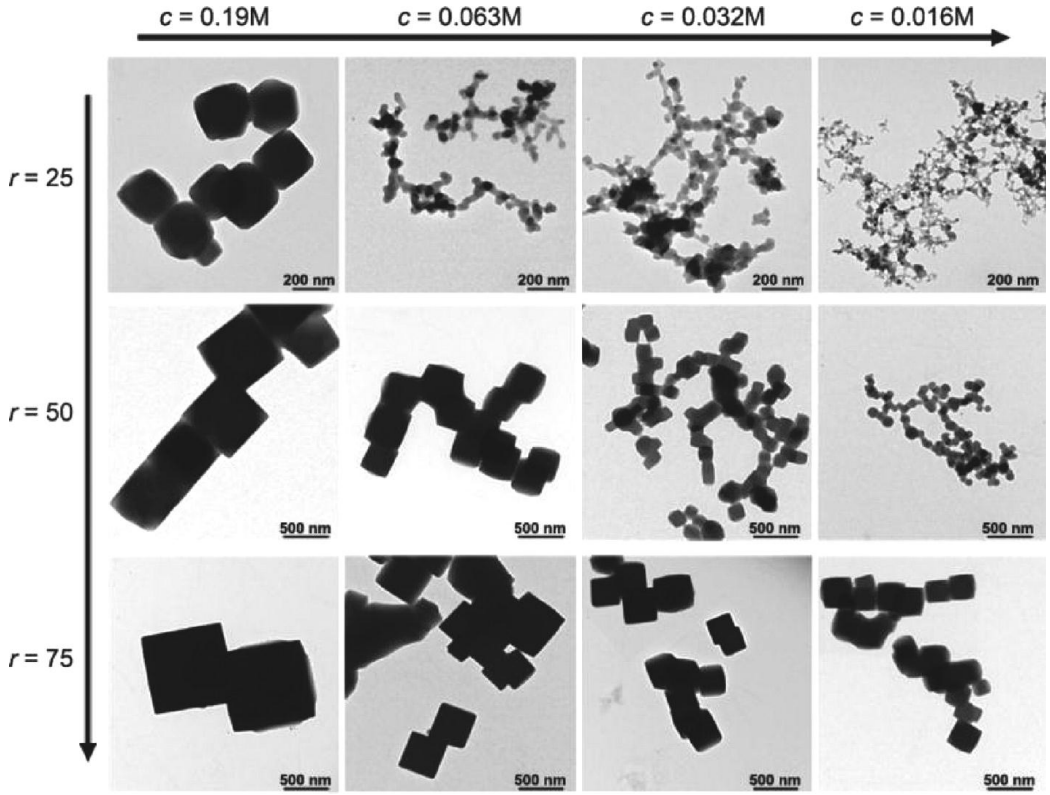

Figure 1.29 TEM micrograph of samples with different concentrations of H_3BTC and dodecanoic acid in microwave radiation at 140 ºC for 10 min [Diring et al., 2010].

Qiu et al. synthesized [Zn(BDC)(H_2O)] nano–sheets, nano–porous framework of [$Cu_3(BTC)_2$], [$Zn_3(BTC)_2 \cdot 12H_2O$] and [Tb(BTC)(H_2O)$_6$] nanowires [Li et al., 2009, 2008; Qiu et al., 2008]. Thereafter Jin et al. synthesized hierarchical architectures of gadolinium 1,4–benzenedicarboxylate by ultrasonic–assisted solution phase technique (Figure 1.30), and studied the factors affecting the morphology of [$Gd(BDC)_{1.5}(H_2O)_2$], i.e. ultrasonic power and time, amount of PVP and concentration of $Gd(NO_3)_3 \cdot 6H_2O$, Na_2BDC. On the basis of extensive structural and theoritical investigations, they have proposed the mechanistic fabrication of these hierarchical architectures [Jin et al., 2012].

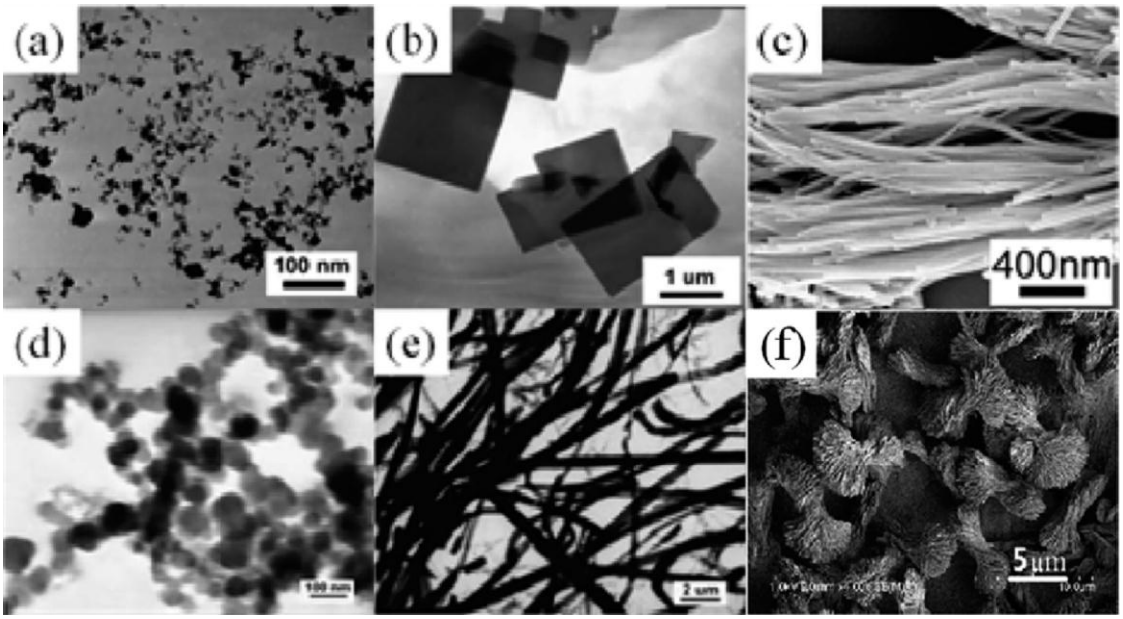

Figure 1.30 SEM micrograph of [$Cu_3(BTC)_2$] nanoparticles (a) [Li et al., 2010], Zn(BDC)(H_2O) nanoplates (b) [Li et al., 2008], [Tb(BTC)(H_2O)$_6$] nanowires (c) [Hu et al., 2012)], $Zn_3(BTC)_2 \cdot 12H_2O$] nanoparticles (d), nanowires (e) and straw–sheaf like (f) hierarchical architetures of [$Gd(BDC)_{1.5}(H_2O)_2$ [Jin et al., 2012].

1.10.4 Nano–Coordination Polymer (NCP) Networks Applications

1.10.4.1 Sensors

Luminescence is one of the most fascinating properties of NCPs, composed of organic ligands with conjugate effect and d^{10} transition metal (Cd^{2+}, Zn^{2+} etc.) or rare earth metals (Tb^{3+}, Eu^{3+} etc.). Nano coordination polymers can be functionalized to bind selectively or identify specific moiety due to their porous structure and larger surface area, and thus can be used as effective sensors [Li et al., 2008; Hu et al., 2012; Yang et al., 2012; Zhang et al., 2011]. Qiu et al. have shown that [$Zn_3(BTC)_2 \cdot 12H_2O$] nano–sized crystals exhibit high selectivity for ethylamine sensing in acetonitrile solution, while [$Tb(BTC)(H_2O)_6$] nanowires display strong luminescence emissions at 492 nm and 548 nm, and exhibit high selectivity for aromatic amines sensing, e.g. aniline and *p*–phenylenediamine [Qiu et al., 2008]. Zhang's group reported the luminescence property of nanostructured CPs [$Tb(BTC)(H_2O)_6$], when dispersed in water and leading to a suspension that retain its inherent stability in an aqueous environment for the highly sensitive and selective sensing of metal ions in acetone and aqueous solution (Figure 1.31) [Yang et al., 2012].

1.10.4.2 Magnetic Resonance Imaging Contrast Agents

NCPs are potential candidates to serve as contrast agents since they can be composed of highly paramagnetic ions, e.g. Mn^{2+} and Gd^{3+}; and their small size permit to several bio–distributions and prospects beyond the conventional imaging through chemical agents [Rocca and Lin, 2010; deKrafft et al., 2012]. Lin et al. have developed the first MRI contrast agent of nano–sized coordination polymers, Gd^{3+}–carboxylate materials. They fabricated [$Gd_2(BDC)_3(H_2O)$] with ~40 nm diameter and 100 nm length

showing exceptionally high transverse and longitudinal relaxivities of 55.6 s^{-1} and 35.8 s^{-1} per mM of Gd(III), whereas $[Gd_2(BDC)_3(H_2O)]$ of ~100 nm diameter and 1 μm length has transverse and longitudinal relaxivities of 45.7 s^{-1} and 20.1 s^{-1} per mM of Gd(III) (Figure 1.32) [Rieter et al., 2006]. Furthermore, Horcajada et al. developed a nanostructured coordination framework constructed from Fe^{3+} metal ions with fumarate ligand that exhibits a longitudinal relaxivity of 50 s^{-1} per mM of Fe^{3+} [Horcajada et al., 2010].

1.10.4.3 Drug Delivery

Nano–coordination polymers are a better alternative for controlled release of therapeutic agents. Lin and coworkers have developed porous MIL–101 (Fe) nano fabricated from Fe^{3+} and 2–aminoterephthalic acid where the amino groups present on MIL–101 (Fe) nanoparticles facilitates covalent interactions to 1,1–carbonyldiimidazole activated ethoxysuccinato–cisplatin pro–drug (Figure 1.33) [Pashowet al., 2009]. More recently, Gref and coworkers designed various nano–structured coordination polymers of carboxylate ligands to load a broad range of antitumoral drugs e.g. cidofovir, busulfan and doxorubicin [Horcajada et al., 2010].

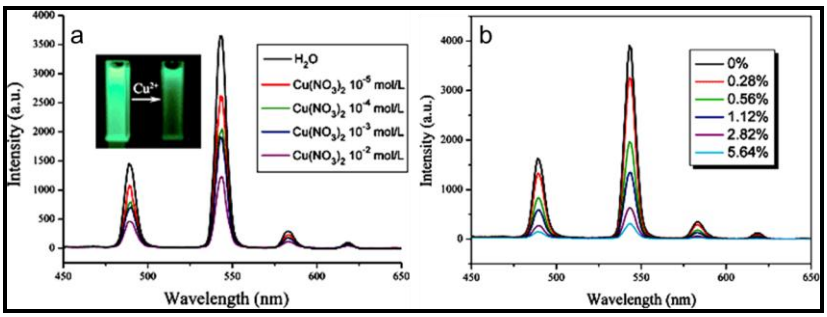

Figure 1.31 (a) The luminescence spectra of $Tb(BTC)(H_2O)_6$ in $Cu(NO_3)_2$ aqueous solution at various concentrations (excition wavelength 300 nm). (b) The emission spectra of $Tb(BTC)(H_2O)_6$ aqueous suspension in the presence of various acetone contents (excitation wavelength 300 nm) [Yang et al., 2012].

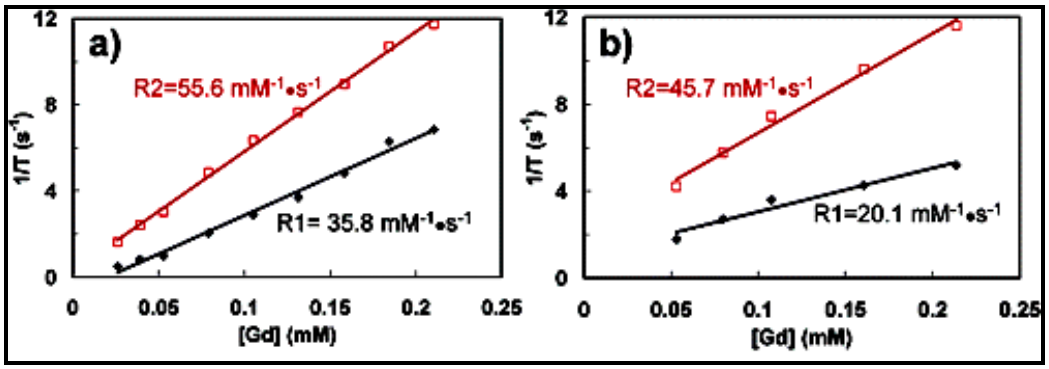

Figure 1.32 (a) Longitudinal and transverse relaxivity curves of $[Gd_2(BDC)_3(H_2O)]$ of ~ 40 nm diameter and ~100 nm length (b) Longitudinal and transverse relaxivity curves of $[Gd_2(BDC)_3(H_2O)]$ of ~ 40 nm diameter and ~100 nm length [Rieter et al., 2006].

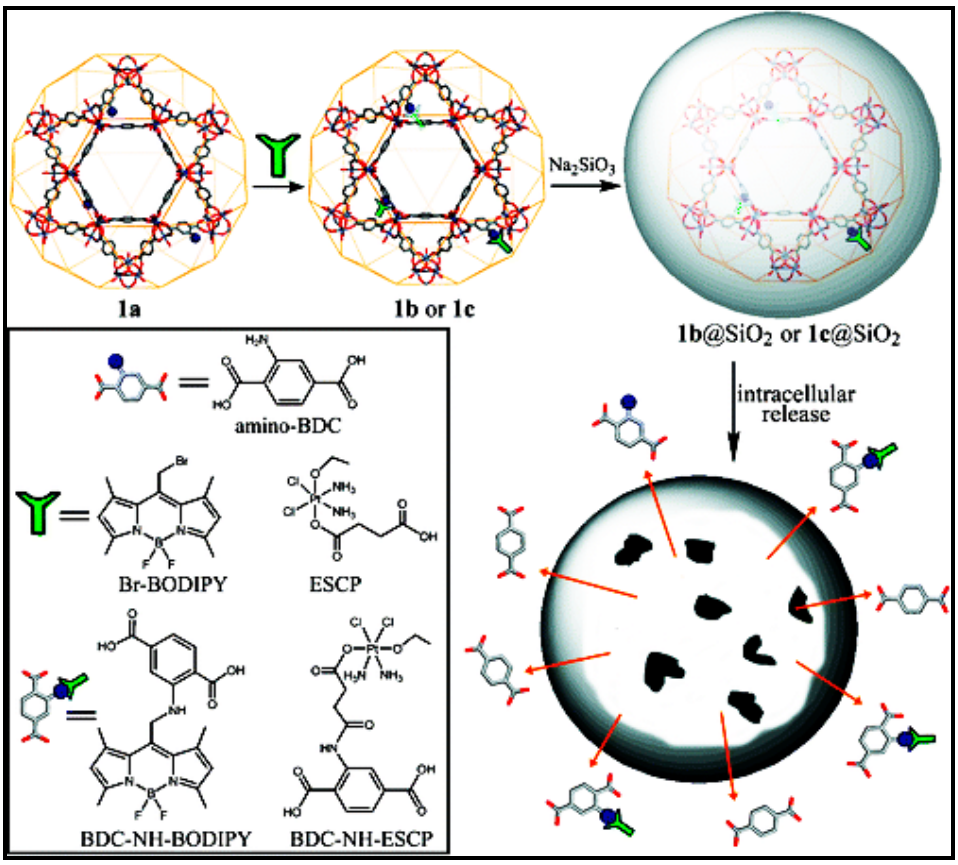

Figure 1.33 Schematic representation of the post–synthetic modification of MIL–101(Fe) nano with a chemotherapeutic agents, successive silica coating and their intracellular release [Pashowet al., 2009].

1.10.4.4 Gas Sorption Properties

Several NCPs of carboxylate ligands with high gas sorption ability are reported e.g. MIL–101, MOF–5 and HKUST–1 etc. Nano–sized porous coordination framework exhibit enhanced, and fascinating gas sorption properties compared to their bulk counter parts. For instance, Bai and coworkers explored MOF–5 nano–cube for enhanced heat of adsorption and larger CH_4, H_2 and CO_2 absorption at room temperature rather than its bulk counterpart. Sun and coworkers developed nano–scopic thermally stable framework of [Al(OH)(NDC)] (H_2NDC=1, 4–naphthalenedicarboxylic acid capable of larger CO_2 and H_2 absorption with excellent selectivity for CO_2 over O_2 and N_2 [Zhang et al., 2012]. Oh and coworkers explored H_2BDC and In^{3+} based NCPs which exhibit CO_2 and H_2 uptake of 333 and 140 cm^3 g^{-1} respectively [Cho et al., 2008]. In addition to that, Kitagawa el al. synthesized homogeneous nano sized crystal of [Zn(ip)(BPY)] (here ip = isophthalate and BPY = 4,4'–bipyridyl) through non–aqueous inverse microemulsion and then ultrasonication. The methanol adsorption experimentation confirmed that although the adsorption ability of both, nano–sized and bulk materials are nearly same, but the sorption isotherm varies dramatically and the adsorption kinetics enhances remarkably [Tanaka et al., 2010].

1.10.4.5 Catalysis

NCPs are potential materials in heterogeneous catalysis mainly for "metal nanoparticles deposition into their pores" due to the chemical tenability, high surface area and porosity [Jiang and Xu, 2011; Meilikhov et al., 2010]. Several pioneering studies are reported for metal nano particles/bimetallic alloy nanoparticles placed at

coordination framework in heterogeneous catalysis [Lu et al., 2012; Kuo et al., 2012]. Qiu and coworkers developed Au/MIL–100 (Fe) porous and core shell nano–catalyst through step wise method and demonstrated its catalytic properties. The improved catalytic activity of the nano–catalyst Au/MIL–100(Fe) rather than Au nanoparticles is due to the synergistic effect [Ke et al., 2013].

1.11 Drug Sensing

Several lifesaving drugs are frequently used in our daily life which cure the diseases and provide us a healthy lifespan. In pharmaceutics, the analytical study of drug materials, the intermediates formed in their synthesis, products, impurities, drug formulations, degradation products and pharmaceutical samples possessing drug and its metabolites is crucial area of research. From the aspect of public health, this investigation is essential to contribute a maximal efficacy, high quality, economic and safety drug therapy during drug production. Therefore a trustworthy technique is necessary for the rapid, accurate and adequate assay of these drugs.

1.11.1 Important Methods for Drug Sensing

The formulation of drugs has a revolutionary impact in the human health. These drugs have intended functioning if they are indexed to an appropriate amount and the impurities are absent. In order to employ the drugs in an efficient way several analytical procedures were endorsed in the quantification of drugs. The drugs to be employed may produce undesired impurities in the steps of their formulation, transport and storage, leading the drugs risky to be addressed; therefore investigation of low–concentration of drugs in complex biological matrixes is necessary in the production and implication of

drugs. Recent drugs have high potency thus required low doses screening of these drugs and their metabolites are great deal of attention; in this view, analytical techniques play a crucial role. Several analytical approaches for drug quantification in bio–samples have been addressed which are discussed below.

1.11.1.1 Titrimetric Techniques

It is one the oldest technique for analysis. The terminology of titration got originated after the invention of volumetric method by Gay–Lussac. This technique is quite advantageous in kinetic measurements which are important for the reaction rate determination. This is used for the assay of captopril [Rahman et al., 2005], albendozole [Basavaiah et al., 2003] and gabapentin [Sameer et al., 2011] in the commercial doses. Similarly Marona et al. determined sparfloxacin by the non–aqeous titration [Marona et al., 2001].

1.11.1.2 Chromatographic Techniques

1.11.1.2.1 Thin Layer Chromatography

Thin layer chromatography (TLC) is an old method and is widely used in the quantitative analysis. In this method, the adsorbent is floored onto a solid holder of plastic, glass or aluminum. There are various parameters that affect the efficiency of chromatography such as selectivity of adsorbent, elusion rate etc. TLC is effectively employed for the assay of unknown substances in bulk amount of drugs [Szepesi et al., 1996]. This technique is employed in the assay of pioglitazone [Gumieniczek et al., 2004], steroids [Cimpoiu 2006], noscapine [Ashour et al., 2009] and celecoxib [Bebawy et al., 2002] including the impurities of drugs [White et al., 1992].

1.11.1.2.2 High Performance Thin Layer Chromatography (HPTLC)

HPTLC is a quick separation technique and it examines the whole chromatogram with several parameters. Additionally it is a detection technique for multiple samples simultaneously and individually. A number of drugs such as ethinyl estradiol, cyproterone [Pavic et al., 2003], alfuzosin [Fayed et al., 2006], tramadol and pentazocine [Ebrahim et al., 2011] have been estimated using HPTLC.

1.11.1.2.3 High–Performance Liquid Chromatography (HPLC)

It is an advancement of liquid chromatography utilized for the separation of individual molecules in the complex mixtures of bio–chemical systems. For the first time it was employed for the estimation of drugs in bulk in 1980 [U. S. Pharmacopoeia, 1980] and later on it became popular in U. S. Pharmacopoeia; 2004, it was also employed in the European Pharmacopoeia and Council of Europe; 2002. Although we have to pay quite high cost in order to get high precision with good specificity in the broad ranging systems. In view of the reported literature it is speculated that HPLC is extensively used chromatographic technique.

1.11.1.2.4 Gas Chromatography (GC)

In the series of chromatographic techniques, it is a potent estimation technique for the assay of volatile organic materials. The combination of simultaneous separation and estimation leads to a precise detection of complex mixtures along with ppm traces of materials. GC has been employed for quantification of various drugs isotretinion [Lima et al., 2005], cocaine [Zuo et al., 2004] including residual solvents

[Somuramasami et al., 2011] and impurities of drugs [Frost et al., 2003; Hiriyanna and Basavaiah, 2008].

1.11.1.3 Spectroscopic Techniques

1.11.1.3.1 Spectrophotometry

Spectrophotometric technique is mainly based on the absorption or transmission property of compounds with respect to wavelength. The assay of drugs using UV–Vis spectrophotometry is increased in recent years [Tella et al., 2010; Venugopal and Sahi, 2005; Sharma et al., 2008]. Colorimetric techniques are mainly used for the quantification of bulk substances. For instance, the assay of corticosteroid drug constitution is utilized by blue tetrazolium determination [Gorog and Szasz, 1978; Gorog, 1983] and quantification of cardiac glycosides (Europian Pharmacopoeia).

Derivative spectroscopy is also utilized for the quantitative assay; it depicts first or higher order derivatives of absorbance as a function of wavelength. Although, the methods is not well explored due to the complexation in the derivative spectra of recent UV–Vis spectrophotometers. The derivative technique has proficient applications in UV–Vis spectrophotometry as well as IR [Mc William, 1969], fluorimetry [O' Haver, 1976; John and Soutar, 1976] fluorescence spectrometry, atomic absorption [Konstantianos et al., 1994; Snelleman et al., 1970]. These spectra are advantageous in case of complex spectra. The limitation of this method is the degradation of signal–to–noise ratio in differentiation [O'Haver and Begley, 1961].

1.11.1.3.2 Near Infrared Spectroscopy (NIRS)

It provides multiple quantification of combination of drugs. Several reports are available for the quantitative screening of active constituents in tablets [Alvarenga et al., 2008; Ramirez et al., 2001; Moffat et al., 2000; Buchanan et al., 1996; Merckle and Kovar, 1998; Thosar et al., 2001; Blanco et al., 1996, 1999, 2000; Li et al., 2003; Molt et al., 1996; Eustaquino et al., 1998; Traford et al., 1999; Corti et al., 1999; Chen et al., 2001]. Additionally, Luypaert et al. and Blanco et al. have published a number of review articles for the drug screening using NIRS [Luypaert et al., 2007; Blanco et al., 1998].

1.11.1.3.3 Nuclear Magnetic Resonance Spectroscopy (NMR)

Initial report for drug assay using NMR technique was published by Shuker et al. [Shuker et al., 1996]. Progressively, several states of art reports are published and covered a broad spectrum in academic research and pharmaceutics. The quantitative assay of impurities associated with drugs has been discussed in precise drugs screening reports and reviews [Reinscheid, 2006; Salem et al., 2006; Martino and Holzgrabe, 2011].

1.11.1.4 Fluorimetry and Phosphorimetry

Fluorescence spectrometrometry is mainly used for the evaluation of micro samples and a number of articles has been published for the quantitative assay [Rahman et al., 2012, 2009]; further phosphorimetric detection is also reported [De Souza et al., 2013; Chaun et al., 2000].

1.11.1.5 Kinetic Analysis Method

This technique involves the investigation of concentration alteration (analyzed by transducer signal) with respect to time when the reactants are mixed. Literature reveals that kinetic analysis technique involves constant time and rate method for the screening of drugs [Darwish et al., 2010; Rahman and Kashif, 2010]. Most commonly used methods for kinetic analysis are continuous reagent addition [Prieto and Silva, 1998] along with fluorimetric [Marquez et al., 1989], photometric [Marquez et al., 1990] and stopped flow techniques [Andrade et al., 2010]. The application of micellar system in kinetic technique improves the reaction rate as well as selectivity and sensitivity thus leading to shorten the analysis time [Monferrer–Pons et al., 1999; Pérez–Bendito et al., 1999; Georgiou et al., 1991]. Multiple kinetic quantification are indexed through differential rate methods [Sultan and Walmsley, 1997]; the H–point standard addition technique [Givianrad et al., 2011] and kinetic wavelength pair technique [Pena et al., 1991] are reported for overlapping and complex spectra.

1.11.1.6 Electrophoretic Techniques

The capillary electrophoresis (CE) is also an important tool for the separation of charged species through a tiny capillary in the presence of electric field. Here the area under the peak provides the quantitative evaluation of concentration. Various reports have been published in drug detection [Nehmé et al., 2010; Zhang et al., 2009; Calcara et al., 2005] and several capillary electrophoretic modes, e.g. micellar electrokinetics chromatography [Hamoudova et al., 2006; Al Azzam et al., 2011; Theurillat et al., 2010], capillary zone electrophoresis [Hamoudora and Pospisilova, 2006; Nevado et al.,

2006; Hauze et al., 2005; Ne´meth et al., 2011; Amin et al., 2012], isoelectric focusing [Lasdun et al., 2001; Liu et al., 1996], capillary gel electrophoresis [Liu et al., 1995; Srivasta et al., 1994], affinity capillary electrophoresis [Li et al., 2011; Martinez–Pla et al., 2004], isotachophoresis [Pospisilova et al., 2005; Kubacak et al., 2005] have been established and employed for purification and quantification of drugs.

1.11.1.7 Flow Injection and Sequential Injection Analysis (FIA)

Ruzicka (U.S.) and Hansen (Denmark) established this method for chemical analysis [Ruzicka and Hansen, 1975; Stewart et al., 1976]. Chemical analysis is carried out by this technique using automation concept based on the measurements executed in the presence and absence of chemical and physical equilibria [Ruzicka and Hansen, 1988; Valcarcel and Luque de Castro, 1987; Karlberg and Pacey, 1989]. The liquid analyte is introduced into a non–sectioned moving stream of suitable liquid. The employed analyte creates a zone that is transported to transducer that tracks the variation in electrode potential and absorbance etc. Various review articles are published exploring FIA monograph of drug quantification [Calatayud and Garcia Mateo, 1992 a,b; Evagen'ev et al., 2001; Fletcher et al., 2001].

1.11.1.8 Hyphenated Techniques

This technique is the integrated form of separation method and on–line separation method. Enormous hyphenated methods, e.g. CE–MS [Blasco et al., 2009] LC–NMR [Lindon et al., 2000], GC–MS [De Lima Gomes et al., 2011] LC–MS [Qian et al., 2012, Wang et al., 2012], CE–ICP–MS [Timerbaev et al., 2012] are introduced for the screening of drugs.

1.11.1.9 Electrochemical Techniques

It is a facile, rapid and effectively precise technique for the assay of a broad spectrum of drugs including their pharmaceutical formulations and real sample investigations. The electrochemical techniques progress the screening of drugs across the existing limitations of other analytical tools. The advantage of this method includes simple handling, low cost, short analysis time and labor consumption, high sensitivity with excellent specificity and ultra–trace detection limit. Several electrochemical methods are employed for the detection of drugs. Titanium dioxide nanoparticles and amberlite XAD–2 modified carbon paste electrode (CPE) is developed for the estimation of trimipramine, imipramine and desipramine, using impedance spectroscopy, CV, DPV, and chronocoulometry [Sanghavi and Srivastava, 2013]; similarly *p*–chloranil modified CPE or capsaicin/carbon nano tube (CNT) modified pyrolytic graphite electrode are formulated for the assay of lidocaine and benzocaine. A silver nanoparticles and copper(II) complex modified CPE are employed for the assay of norepinephrine, dopamine, epinephrine and levodopa using chronocoulometry, impedance spectroscopy, stripping voltammetry and cyclic voltammetry (CV) [Sanghavi et al., 2013]. The electrochemically synthesized capsaicin–benzocaine adduct induces a linear decrement in the voltammetric signature of capsaicin related with the added benzocaine concentration [Kachoosangi et al., 2008]. Adsorptive stripping DPV technique is used for the assay of desvenlafaxine and venlafaxime by nafion/CNT modified GC (glassy carbon electrode) [Sanghavi and Srivastava, 2011b]. Cryptand and CNT based CPE is introduced for the nanomolar detection of bismuth using potentiometric stripping technique [Gadhari et al., 2010]. Sanghavi and coworkers have

quantified in situ aspirin, acetaminophen and caffeine separately and simultaneously with CNT modified electrode [Sanghavi and Srivastava, 2010]. The potentiometric stripping investigation is introduced to estimate antimony using rice husk and hexathia crown ether modified CPE [Gadhari et al., 2011]. An effective and fast screening of bensevazide, levodopa and its impurity in co–beneldopa dosages through capillary electrophoresis by amperometry is developed [Wang et al., 2005].

1.12 Electrochemical Sensing of Drugs

Enormous sensitive techniques have been developed for the effective quantification of drugs such as titrimetry, chromatography, spectrophotometry, fluorimetry and phosphorimetry, hyphenated techniques, flow injection, sequential injection analysis, electrophorety, and nuclear magnetic resonance spectroscopy (NMR) etc. Although these techniques are time consuming and need costly equipment and sophisticated instrumentation [Narang et al., 2015]. Electrochemical sensing is an advantageous, versatile, and powerful analytical technique which is adjustable to any device in the aspect of its sensitivity, selectivity and portability towards several target analytes. After development of further sensitive pulse techniques, the electrochemical investigations are more frequently employed on environmental, industrial applications, drug detection and their commercial formulation, particularly detection of drug candidates in the biological samples. Furthermore, electrochemical techniques can easily handle enormous issues of pharmaceutical interest in a highly accurate, sensitive, precise and selective approach. Additionally it offers rapid, facile, simple and cost effective on the spot detection tool without compromise in the sensitivity and selectivity. Some of the most useful electroanalytical methods are based on the concept

of varying the applied potentials to the electrode–electrolyte solution and measuring the resulting current [Hallam et al., 2010]. Most of the materials are found to be electro–active and therefore there has been huge acceleration in advancement of the sensitive electrochemical analysis [Uslu and Ozkan, 2011; Farghaly and Ghandour 2005]. In recent years many efforts has been made in order to improve the sensitivity of electrochemical sensors.

Voltammetry is a class of electrochemical technique, which is employed to designate the current–voltage measurement obtained at a given electrode. It is based on voltage–current–time relationship in the three electrode system, reference electrode, working electrode and auxiliary electrode. This relationship could be explained when potential is applied to the working electrode and the resultant current flowing through the cell will be recorded. The potential could be changed or resulting current will be recorded over a period of time. The applied potential applied to the working electrode acts as a driving force and controls the redox reaction of the chemical species. In this aspect, DPV is an interesting category of voltammetry, it consist a series of potential pulses of increasing amplitude. The potential is fixed and it is superimposed on slowly varying base potential, the peak current is measured at two points; before application and at the end of each pulse [Wang, 2000]. The first current is subtracted from second and the current difference is plotted against the applied potential. The largest peak current is proportional to the concentration of analyte. This technique quantifies the drug concentration in a very precise way.

1.12.1 Interesting Examples of Electrochemical Sensing of Drugs

The electro–oxidation of metoclopramide hydrochloride [Wang et al., 2001] is studied and it is executed by second derivative adsorptive anodic stripping voltammetry by a glassy carbon electrode modified with nafion. The peak current is proportional to analyte in the concentration range of 0.5–154.5 ng mL^{-1} with a detection limit of 0.027 ng mL^{-1}; the test was also performed in human serum. The electrochemical behavior of norfloxacin [Ghoneim et al., 2001] on a glassy carbon electrode in acetate buffer of pH 5.0, is studied; it gives a sensitive oxidation peak at 0.9 V. Further the norfloxacin measurement is performed in biological fluid with a linear calibration curve in the concentration range of 5–50 μg mL^{-1} and limit of detection 1.1 μg mL^{-1}. The assay of isoniazid (INH) and rifampicin (RIF) combined and separately accomplished at CPE in pharmaceutical formulation and human serum [Hammam et al., 2004]. The simultaneous detection of both drugs in human serum provides the assay and limit of detection of 5×10^{-8} M for RIF and 6×10^{-8} for INH.

A systematic study for the detection of Cephalosporins (cefobid and rocephin) was executed by various voltammetric techniques [Maali et al., 1993; Özkan et al., 2000]. Sulfadiazine was quantified in artificial intestinal and gastric juices *via* differential pulse voltammetry [Zunino et al., 1987]. However sulphamide was detected by indirect differential pulse voltammetry [Fogg and Ahmed, 1974] depending on coupling and diazotization between sulfonamide and 1–naphthol in alkaline medium.

Liu et al. have synthesized nitrogen doped porous carbon nanopolyhedrons (*N*–PCPs) and multi–walled carbon nanotubes hybrid material; they employed this material for the simultaneous electro–detection of phenols (catechol, hydroquinone and

resorcinol) in the linear concentration range of 0.7–440 μM, 0.2–455 μM, and 3.0–365 μM with detection limits 0.11μM, 0.03 μM and 0.11 μM respectively [Liu et al. 2013]. Glassy carbon electrode coated with multi–walled carbon nanotubes was employed for the electrooxidation of resorcinol in Britton–Robinson (B–R) buffer pH 6 through various voltammetric methods [Ghoreishi et al., 2011]. The calibration curve of electrodetection provide the linear relashionship in the concentration range of 1.2×10^{-6} to 1.9×10^{-4} with detection limit 1.1×10^{-6} M and 4.9×10^{-7} M at S/N 3 for square wave and differential pulse voltammetry. Enache and Brett have performed systematic study for the electrochemical behavior of hydroquinone, catechol and resorcinol along with some para–substituted phenolic compounds (tyrosine, 4–ethylphenol and tyramine) at GC electrode in a wide range of pH [Enache and Brett, 2011]. They proposed the pathway for the electrochemical oxidation of these compounds. We have developed voltammetric method for the highly sensitive ultra–trace detection of resorcinol in a wide range of concentration. The sensitivity and limit of detection is found to be 0.019 μA/nM and 29.77 nM respectively at S/N 3.

The forensic detection of atropine was executed electrochemically by Ramdani et al. using economic screen printed and disposable graphite sensors in buffer solution of pH 10. The limit of detection for the developed sensor is 3.9 mM (based on S/N 3) in the concentration range of 5 mM–50 mM. The practical utility of the developed method is demonstrated through a systematic strategy of determination in coca–cola [Ramdani et al., 2013]. Li et al. designed a *β*–cyclodextrin modified ion sensitive field effect transistor sensor for atropine detection over the concentration range of $5.0\times10^{-3}-1.0\times10^{-6}$ mol/L and the pH range of 5.0－8.5. The sensor detection limit was

8.0×10^{-7} mol/L. They also studied the response curve, pH influence, life and stability of the sensor [Li et al., 2005]. In this series, Atta et al. prepared platinum electrode modified with poly (3,4–ethylene–dioxythiophene) (PEDOT) electrode film in presence of sodium dodecyl sulfate (SDS) for the electrochemical detection of anticholinergic drug, atropine sulphate along with morphine using linear sweep voltammetry, cyclic voltammetry and electrochemical impedance spectroscopy in B–R buffer. The method is also verified in the assay of atropine sulphate in injection in the linear ranges of 0.1 to 0.8 μmol L^{-1} with low detection limits of 27 nM [Atta et al., 2012]. Dar et al. have developed atropine sensor in presence of anionic surfactant media, sodium benzene sulfonate (SDBS) and supporting electrolyte, tetramethyl ammonium hydroxide pH 10.5 at handmade multi–walled carbon nanotube electrode which provides the linear response in of atropine concentration range from 3.98 ng/ml to 27.23 ng/ml with detection limit 0.449 ng/ml. Further, the analysis was verified practically in pharmaceutical formulation of ophthalmic solution (eye drop) [Dar et al., 2011]. Bagheri et al. proposed a strategy for the direct detection of atropine in complex matrices at CPE modified with Co_3O_4–graphine [Bagheri et al., 2015]. The linear calibration curve for atropine concentration lies in the range from 0.1–3.2 μmol L^{-1} with the detection limit of 0.03 μmol L^{-1}. Further, the analytical performance of the developed sensor is examined practically by determining atropine in biological fluids and pharmaceutical samples [Bagheri et al., 2015]. We have fabricated the atropine sensor by modification of carbon paste electrode with nano–porous coordination polymer DMTD–Ag which facilitates the trace level detection with sensitivity and limit of detection as 0.02 μA/μM and 46.00 nM in a wide concentration range. Further,

practical implementation of developed method is verified by atropine detection in pharmaceutical formulation, eye drop.

Ghamdi et al. have quantified ciprofloxacin (CFX) at hanging mercury dropping electrode (HMDE) in B–R buffer pH 2.5 [Ghamdi et al., 2014]. The monitored anodic peak current was proportional to the concentration of CFX, where it revealed a linear response in the range 3.0×10^{-7}– 2×10^{-6} M detection limit of 7×10^{-9} M. They also verified the proposed method by CFX assay in its pharmaceutical formulation and spiked human urine. Diab et al. investigated the voltammetric behavior of CFX at unmodified GC electrode and DNA modified glassy carbon electrode through differential pulse voltammetry and cyclic voltammetry. There is a linear relationship between anodic peak current and ciprofloxacin concentration in the range 1–10 μM with detection limit of 0.117 μM [Diab et al., 2013]. Osman et al. synthesized spinel structured $Ba_{0.5}Co_{0.5}Fe_2O_4$ nanoparticles by glycol thermal technique [Osman et al., 2015]. The electroactivity of nanoparticle was employed in the electro–detection of CFX in a linear range 1.0×10^{-8} – 0.5×10^{-3} M and a detection limit of 5.8 nM. Furthermore, possible interference by several excipients usually present in pharmaceutical formulations was evaluated. Cai et al. prepared a nano–SnO_2/PVS film at GC electrode and they quantified CFX at modified electrode [Cai et al., 2007]. In addition to the electrochemistry, spectroscopic methods and agarose gel electrophoresis techniques were also employed to examine the interaction of CFX and calf thymus DNA. We have executed schematic study for the electrochemical detection of CFX at AMT–Ag modified CPE in phosphate buffer pH 7 which provides significantly low detection limit of 5 nm with sensitivity 0.001 μA/μM at signal–to–noise ratio (S/N) 3.

Further the method is practically validated by CFX detection in pharmaceutical pharmulation (ophthalmic solution) and biological fluid.

1.13 Scope of the Work

The research in the area of nano–porous coordination polymers and nano–crystalline coordination polymers is not well explored as evident from the bar diagram based on the available SciFinder reports from 2005–2015. Here, the ligand plays a crucial role in the fabrication of coordination polymer assembly. In this aspect DMTD and AMT have feasible functionality and active sites for the development of novel nanocoordination building blocks. Therefore, apart from the development of novel synthetic routes for AMT and DMTD endowed metal nanocoordination polymers, the other applications of these nanoscale materials are also thoroughly studied.

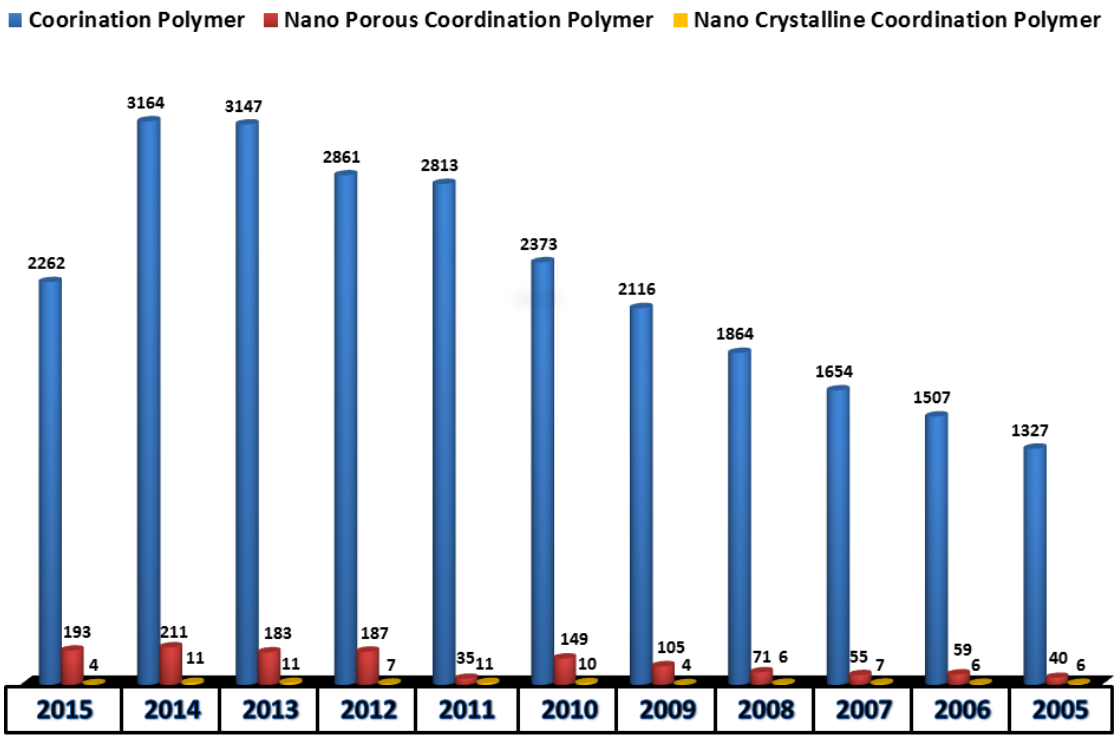

Figure 1.34 Annual literature available in coordination and nano–coordination polymer based on SciFinder reports.

Significant work needs to be executed in order to explore the applications of nanocoordination polymers for practical applications. In view of these issues, this thesis thoroughly discussed and provide a crystal clear perspective on the development of nanostructured coordination polymers derived from 2–mercapto–1,3,4–thiadiazole based ligands with silver and gold ions. The Ag and Au form prominent and fascinating networks with organic ligands and have tremendous implications in the drug sensing. The developed frameworks are applicable in voltammetric assay of atropine sulphate, ciprofloxacin hydrochloride and their pharmaceutical formulations. It is worthy to mention that it is for the first time to report the electrochemical applications of these assemblies in drug sensing. These frameworks can be efficiently utilized in various catalytic and electrosensing applications.

1.14 Objective of the Thesis

The objective of the thesis is firstly to optimize the reaction conditions for the synthesis of coordination polymer networks with Au(I) and Ag(I) using the unique and highly stable ligands 2,5–dimercapto–1,3,4–thiadiazole and 2–amino–5–mercapto–1,3,4–thiadiazole; and secondly to employ these developed motifs in the electrochemical ultra–trace detection of life–saving drugs.